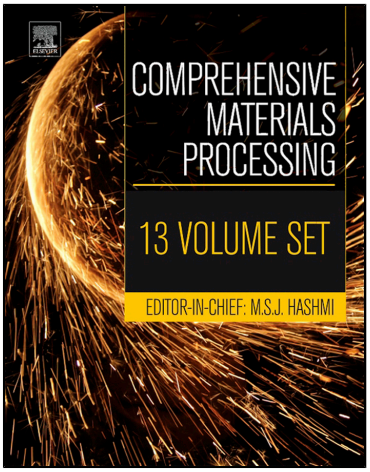

From Zuliani, C.; Curto, V. F.; Matzeu, G.; Fraser, K. J.; Diamond, D. Properties and Customization of Sensor Materials for Biomedical Applications. In Comprehensive Materials Processing;Hashmi, S., Ed.; Vol. 13; Elsevier Ltd: Elsevier, 2014; pp 221–243.
ISBN: 9780080965321

13.09 Properties and Customization of Sensor Materials for Biomedical Applications

C Zuliani, VF Curto, G Matzeu, KJ Fraser, and D Diamond, Dublin City University, Dublin, Ireland

13.09.1 Introduction

13.09.1.1 Key Challenges in Molecular Sensing for Biomedical Applications

Low-power chemo- and biosensing devices capable of monitoring clinically important parameters in real time represent a great challenge in the analytical field as the issue of sensor calibration pertaining to keeping the response within an accurate calibration domain is particularly significant (*1–4*). Diagnostics, personal health, and related costs will also benefit from the introduction of sensors technology (*5–7*). In addition, with the introduction of Registration, Evaluation, Authorization, and Restriction of Chemical Substances (REACH) regulation, unraveling the cause–effect relationships in epidemiology studies will be of outmost importance to help establish reliable environmental policies aimed at protecting the health of individuals and communities (*8–10*). For instance, the effect of low concentration of toxic elements is seldom investigated as physicians do not have means to access the data (*11*).

Implantable devices, which in the past brought much hope for continuous monitoring of chronic medical conditions, have made little progress in the last 20 years. The major mechanism of failure is the biodegradation of the sensing layer and the changing diffusional barrier that arises from the host's response toward the implanted sensor (*12*). Current devices cannot be used for prolonged periods of measurement because of endogenous interferences, fouling, and so on (*13–15*). However, there are few examples of commercially available sensors that are suitable for short-term continuous monitoring of clinical relevant markers.

Comprehensive Materials Processing, First Edition, 2014, 221–243

For instance, the Abbott Freestyle Navigator, which continuously monitors glucose, has been successfully applied for over 5 days in trials (16). In addition, recent work has demonstrated continuous performance of indwelling glucose biosensors for up to 4 months in rats and up to 1 year in pigs (12). However, the ultimate goal of an implantable sensor that would automatically trigger the release of insulin remains very far from realization (17).

From this point of view it is significant to note that glucose sensors account for approximately 85% of the biosensor industry, and that these sensors are based on the employment of enzymes (16). In this regard, the physical and chemical stability of enzymes and their cost often represent a major hurdle in the sensors' development. Therefore, materials that provide a stabilization of the enzymes or that can work as selective catalysts mimicking the proteins function are of outmost importance. In addition, sampling represents another important aspect of consideration in order to deliver minimally invasive sensors and, in this regard, easily accessible body fluids, i.e., sweat, saliva, and interstitial fluids, rather than blood offer a paradigmatic shift in the sampling strategy (18–25). For instance, sweating may assist in the removal of toxic elements, e.g., heavy metals, from the body (11), and the design of robust trials for accessing the analytical levels of these elements in the sweat would help establish therapeutic protocols.

Interstitial fluids have also received attention because of the advantages that this media offers compared to blood, i.e., easily accessible, painless sampling, and reduced risk of infection (12,26–29). However, an important fact often overlooked is that the sample volume of the harvested interstitial fluids is low, i.e., 10 μl h^{-1}. Few examples based on the sampling of interstitial fluids have actually been reported and, even for glucose, a commercial device that can reliably monitor its concentration appears elusive. To date, there is no unanimous agreement on the typical delay between the glucose levels measured in interstitial fluids and whole blood samples (14,28–30). Microspikes and hollow microneedles have been employed to harvest the interstitial fluids, and the integration of these structures with a sensor in a microfluidic device is an attractive possibility. For example, Trzebinski et al. (27) functionalized the top layer of a microspike array suitable for piercing the skin with an enzyme layer allowing the detection of glucose or lactate in buffered solutions. However, using functionalized solid microneedles array for *in vivo* sensing is challenging because of the potential structural deformation upon their insertion into the skin, which, for instance, may drastically change the sampling dynamics, thereby introducing an unpredictable delay in the time from sampling to detection.

The integration of on-body sensors into textiles allows monitoring physiological parameters in a noninvasive fashion, and it has generated considerable research activity across many important biomedical applications such as sports, exercise, and personal health (31). At present, only wearable electrodes to monitor heart rate (32) and wearable respiration devices are commercially available, and the goal of producing reliable chemical-sensing garments seems largely unmet (33). Producing wearable chemical sensors, which must be comfortable during daily activities, reliable, and available at affordable cost, is a challenging task (34). In addition to these challenges, population growth and aging population profiles will significantly affect the cost of health care systems, and the future sustainability of healthcare services will rely on the adoption of new low-cost technologies, with the shift to much more personalized and home or community-based healthcare systems (19,35–38).

13.09.1.2 An Outline of Clinical Markers

13.09.1.2.1 Molecular Clinical Markers

The concentration of ethanol in blood is strictly regulated, and the breath analyzers market has successfully matured in order to enforce drink-driving legislation. However, it is interesting to note that the ethanol level in sweat has a significant clinical relevance as it correlates well with its concentration in blood (31). Lactate concentration in blood is a fundamental parameter for the diagnosis of clinical disorders such as hypoxia and drug toxicity (39). It also gives information on the extent of hemorrhagic shock in trauma patients (12) and of myocardial ischemia (10,13,40–42). In sports science, lactate levels in blood are measured in order to determine the so-called anaerobic threshold, which is a fundamental aspect in optimizing athletes' training (10,43–45). Therefore, there is considerable interest in developing less-invasive, real-time devices for the measurement of lactate in sweat and saliva, as the lactate concentration correlates with that of blood (10,31,43). While sensors for the determination of lactate in saliva have been reported in the literature (10), a key challenge is their integration in a wearable platform that allows real-time analysis. One example of such a wearable sensor would be the integration into gum shields.

Cholesterol (46) and urea (47) have been standard parameters for the diagnosis of cardiovascular disorders. The development of low-cost sensors for these analytes has received remarkable attention in the literature. Similarly, ammonia sensors have been investigated, especially for point-of-care applications, as high levels of ammonia, which is a product of the urea degradation, are associated with renal dysfunction (48) and other pathologies (49). Interestingly, ammonia concentrations in human breath correlate well with the levels of urea found in blood (50). However, commercial sensors for home-testing or point-of-care are not common and tend to be relatively expensive. For instance, portable ammonia detectors cost more than 400 euro (www.gasmonitor-point.co.uk/ammonia-gas-detectors, www.draeger.com).

In addition, some molecules of interest are difficult to detect, such as bilirubin and nitric oxide. Bilirubin is a tetrapyrrole formed from the breakdown of the heme in red blood cells, whose concentration in blood serum is normally in the 1–10 μM range and is associated with liver functionality (51,52). Nitric oxide (NO) has multiple critical functions in biological systems, e.g., as a neurotransmitter, cytostatic agent, and blood pressure regulator, and it is thought to be implicated in the pathogenesis of several diseases, e.g., gastric tumor. Spectroscopic measurements of bilirubin in blood are difficult because of interferences such as pH effects, and biosensors based on bilirubin oxidase are hampered by the relative instability of the enzyme (51). Studies on NO are further complicated by its chemical reactivity with hemoglobin, oxygen, and other biological species, which results in a half-life ranging from 6 to 50 s (53).

13.09.1.2.2 Ionic Clinical Markers

Monitoring of pH has received attention because of its clinical relevance. For example, pH in sweat may be related to acid build-up in muscle cells during exercise, and pH in wounds may be associated with the wound healing process (54). On-skin pH meters and electrodes can be obtained from Hanna instruments (www.hannainst.co.uk), but they are not designed for continuous monitoring. Levels of sodium, potassium, and chloride in sweat have been used for diagnostics of cystic fibrosis (19,36,55,56). Real-time monitoring of the sweat electrolyte content could also be important for regulating hydration/dehydration issues, which can be fatal in some cases (57,58). The so-called dietary minerals, e.g., Ca^{2+}, Cl^{-}, K^{+}, and Mg^{2+}, have an important physiological role and when present at excessively high and low levels can be harmful for human beings (59–61). For example, calcium has an important role in key biological processes such as the coagulation cascade and regulation of muscular activity, and hypercalcemia is an indicator of the possible presence of malignant tumors (62). Lithium in saliva can be used to regulate lithium carbonate intake during treatment of manic depression and hyperthyroidism disorders (63). Li–ion-selective electrodes (ISEs) are generally sensitive to high sodium concentration (64), but in saliva the sodium levels are three orders of magnitude lower than in blood (65). There is an interest in monitoring ammonium and trace metals in sweat (66). As an example, in people affected by Wilson's disease, copper is absorbed through the intestines and reduced excretion by the liver, causing an accumulation of the metal in the body (66). In addition, copper accumulation maybe connected not only to liver damage (67) but also to Alzheimer's disease (68).

13.09.1.3 Opportunities for Materials Science in Biomedical Sensing

A holistic approach is required to solve the multidisciplinary challenges associated with the preparation of the next-generation biomedical devices, which must be low cost, low power, reliable, and easy to operate. Materials science plays a significant role of delivering suitable materials for such devices, as discussed (69–71). Self-powered sensors will have a key role in the biomedical field. For instance, microfluidic paper analytical devices show promise as low-cost and disposable devices, more so when coupled with paper-based batteries. Liu and Crooks (72) demonstrated the detection of glucose on a paper-based micro-electrochemical sensing platform where the battery is activated by the contact with the sample. The readout is based on the change of color of the electrochromic Prussian Blue spot deposited on the indium tin oxide (ITO) surface, as shown in Figure 1 (72). Such devices would benefit from research in material science as their performance can be optimized; e.g., the paper can be loaded with ionic liquids that may influence the stability of enzyme, or ITO may be replaced by other conductive surfaces, e.g., conductive polymers (CPs) to deal with the forecasted short supply of indium. Perhaps the most important challenge is to understand how to reduce biofouling in implanted sensors. The mechanism of biofouling of implanted systems seems to be related to the denaturation of extracellular matrix proteins, which triggers the inflammatory cascade (73). Materials should be designed to stop or inhibit this initial step.

Phenylboronic acid and derivatives have been extensively exploited as glucose receptors in 'smart' hydrogels as the binding induces a change in the optical diffraction, thus making it possible to monitor minute changes in the hydrogel volume of a microscale device (74). For instance, it was shown that these hydrogels can be used as holographic glucose sensors in simulated tear fluids with negligible interferences from lactate and pH (74). This seems a fascinating approach for noninvasive real-time analysis, and this research seems to have addressed the optimization of the response kinetics.

Stimuli-driven recognition, transportation, and translocation processes perfected by nature over millions of years is surely a source of inspiration (75). For instance, polymer brushes based on a photo-responsive polymers have received much interest as colorimetric sensors due to their ability to report colorimetrically the presence or absence of the ion–ligand complex (76). A photochemically and electrochemically triggered gold nanoparticle sponge has been prepared in Willner's group by attaching spiropyran and thioaniline moieties to the particles (77,78). Interestingly, it was reported that this composite can be used as an

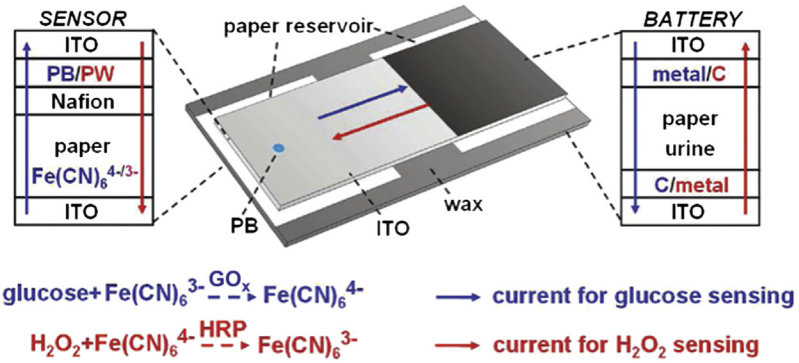

Figure 1 The operational principles of a device consisting of a sensor and an Al/air battery separated by a wax barrier. The paper reservoir of the sensor is preloaded with dried glucose oxidase (GO_x) and $Fe(CN)_6^{3-}$. The catalytic oxidation of glucose by GO_x results in the conversion of $Fe(CN)_6^{3-}$ to $Fe(CN)_6^{4-}$, which is then oxidized back to its original state on the lower ITO electrode, resulting in the reduction of Prussian Blue to colorless Prussian White on the upper ITO electrode. Reprinted (adapted) with permission from Liu, H.; Crooks, R. M. *Anal. Chem.* **2012**, *84*, 2528–2532. Copyright (2012) American Chemical Society.

imprinted matrix for a zwitterionic electron acceptor whose uptake and release is controlled electrochemically and photochemically through the conductive polymer and the spiropyran moieties, respectively (*77*).

Materials that may provide the much-sought-after control of structure at the nanoscale in order to obtain, for instance, larger surface areas, improve electron communication with enzymes and enhance surface plasmon effects are of particular interest (*79*). Ionic liquids, conducting polymers, metal nanoparticles, hydrogels, and hybrids of these materials are appealing from this point of view, and they are discussed in the upcoming sections.

13.09.2 Ionic Liquids and Sensing

13.09.2.1 Introduction to Ionic Liquids

According to current convention, a salt that melts below the normal boiling point of water is known as an ionic liquid (IL) or by one of many synonyms, including low/ambient/room temperature molten salt, ionic fluid, liquid organic salt, fused salt, and neoteric solvent (*80*). ILs have received considerable attention for a wide range of applications, across catalysis reactions, electrochemistry, separation science, polymer chemistry, formulation of pharmaceutical drugs, amongst others (*81*,*82*). The reader is invited to consult several reviews available in the literature to have a wider insight on this matter. For example, Hapiot and Lagrost (*83*) and Buzzeo et al. (*84*) focused on the electrochemical reactivity of ILs, and their properties in relation to fundamental electrochemical studies. MacFarlane and coworkers discussed the chemistry of ILs and how this affects their physicochemical properties (*80*,*85*). Wei and Ivaska (*86*) discussed the application of ILs in electrochemical sensors. Erdmenger et al. (*87*) described the use of ILs for controlling polymerization reactions, while Armand et al. (*88*) outlined future trends of ILs use and applications.

ILs are typically characterized by a bulky, unsymmetrical cation combined with a poorly coordinating anion in order to impede tight packing of the ionic lattice (*89*), and hence the resulting melting point is dramatically decreased compared to conventional salts (*90*). ILs can be classified within seven different families on the basis of the ionic structure (*91*), and typical cations are shown in Figure 2. Their properties depend dramatically on the cation–anion combination (*83*) and in this sense can be thought as 'designer' or 'fine-tunable' (*92*) as polarity, viscosity, thermal stability, conductivity, and solvent capacity can be tailored by thoughtful choice of cations and anions (*85*,*93*). The variation in properties between salts, even those with a common cation but different anions, is dramatic. For example, butylmethylimidazolium hexafluoro-phosphate [C_4mim][PF_6] is immiscible with water, whereas butylmethylimidazolium tetrafluoroborate [C_4mim][BF_4] is water soluble (*94*).

There are several reasons to consider ILs as particularly appealing in the development of biosensors. For example, the existence of nanoscale structural heterogeneities in ILs and in particular the presence of H-bonded nanostructured networks with polar and nonpolar regions has been associated with the stabilization of enzymes (*95*). This very relevant characteristic is discussed more in detail in the next section. In addition, ILs have received attention as they offer good media for the dispersion of carbon nanotubes (CNTs) (*96*), and examples of successful applications of IL–CNTs composites in sensing are discussed in Section 13.09.4.3. Hybrid multiwalled carbon nanotubes-ionogel monoliths (from a silica matrix) show a mixed ionic and electronic conductivity, which makes them potential candidates as electrode materials or electron-to-ion transducers in ISEs (*96*). In some cases, ILs in their solid state have conductivities comparable to the liquid phase, e.g., ethylammonium dicyanamide, which in connection to their plasticity makes them valuable materials as solid-state electrolytes in sensor designing (*97*). Other properties often mentioned are their low volatility, high ionic density, and conductivity (up to 100 mS cm^{-1}), as well as excellent chemical and electrochemical stability (potential windows up to 7 V have been reported) (*98*).

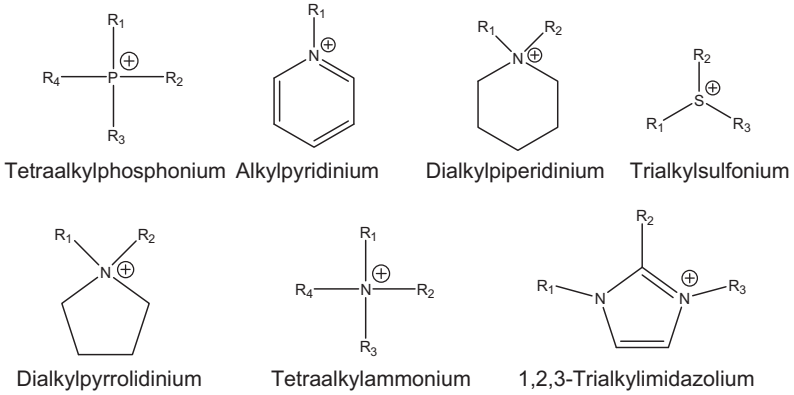

Figure 2 Common cations used for preparation of ILs. Popular side chains include CH_3(Me), C_2H_5(Et), *n*-C_3H_7(Pr), *n*-C_4H_9(Bu), *n*-C_6H_{13}(Hex), *n*-C_8H_{17}(Oct), *n*-$C_{10}H_{21}$(Dec), *n*-$C_{16}H_{33}$(Hexde), $CH_2(OH)CH_2$(HydroPr), CH_3OCH_2(MeOMe), $CH_3OC_2H_4$(MeOEt). The most commonly used anions are BF_4^-, $CF_3BF_3^-$, $CF_3SO_3^-$, $(CF_3SO_2)_2N^-$, PF_6^-, $(CN)_2N^-$, $(CN)_3N^-$, SCN^-, Cl^-, Br^-, $EtSO_3^-$, NO_3^-, $H_2PO_4^-$. Adapted from reference Torimoto, T.; Tsuda, T.; Okazaki, K.; Kuwabata, S. *Adv. Mater.* **2010**, *22*, 1196–1221.

It is worth mentioning some of the drawbacks of ILs as material for sensing to give the reader a wider background. Often overlooked in the ILs literature is their complex chemophysical nature, currently not fully understood, which may complicate prediction and tuning of their role in a sensor. For instance, theoretical models to describe the nonideal conductivity and of the double-layer charging behaviors are yet to be implemented (*83,99*). Second, problems can stem from their relatively high viscosity, cost, and in some cases toxicity (*83,84,99*). For instance, high viscosity impedes the diffusion of solutes and charge transport (*83,84,99,100*), and the ion transport in ILs is limited by the availability of channels of suitable size within the structure. Third, the liquid nature of ILs is a limiting factor in the preparation of point-of-care biosensors because of the additional degree of complexity that liquid sampling brings. In this regard, the introduction of ionogels may offer some solutions as discussed in Section 13.09.5.

13.09.2.2 Ionic Liquids and Biomedical Sensing

13.09.2.2.1 Ionic Liquids in Biosensors

ILs can be employed as a new class of solvents as many biological molecules (proteins, amino acids, DNA, sugars, and polysaccharides) can be solubilized in them without loss of their bioactivity (*103*). This specific property seems to be particularly relevant for the field of biosensing because ILs can provide an effective way to overcome the stability limitations of these sensors related to the limited temperature range and the very narrow pH range for protein stability in water (*88*). An increase in the stability and activity of enzymes has been observed using certain ILs compared to common aqueous media such as phosphate buffer solution (PBS) (*89,101*). For instance, it was reported that cytochrome-*c* can be stored in hydrated choline dihydrogenphosphate for up to 18 months without losing its activity (*102*). Moreover, lysozyme was stabilized against denaturation during thermal cycles in aqueous media containing an equal mass fraction of ethylammonium nitrate while the unfolding/refolding of the protein is not possible when the IL was not added (*103*). Yang et al. (*104*) first demonstrated the use of ILs as electrolytes for the development of organic electrochemical transistors (OECTs) for glucose sensing. These plastic-based devices (*105*) coupled with ILs offer potential advantages for the preparation of low-cost, reliable, and long-term stable biosensors. The mechanism of protein stabilization in ILs is still under debate, but it seems that hydrogen bonding and electrostatic interactions between the IL and the enzyme may increase the kinetic barrier for the unfolding of enzymes (*86,101,106–109*). It is important to note that this is not a general trend in ILs and that some ILs have been known to denature proteins (*83*).

ILs such as *n*-octyl-pyridinium hexafluorophosphate (nOPPF$_6$), which is solid at room temperature, have been employed as a binding agent and mixed with graphite and enzymes to prepare new generations of biosensors. It was found that the carbon to IL ratio strongly influences the performance of the electrode, in that it controls the capacitive current through reduction of water content and it can regulate the electrode conductivity (*110*). For example, Ping et al. (*111*) used nOPPF$_6$ as a binder to create screen-printed graphite ink for the selective detection of dopamine with low interference from ascorbic acid and uric acid. These screen-printed electrodes after the electrochemical deposition of exfoliated graphene oxide and after electrode modification with coating containing glucose oxidase were used to detect glucose in buffer solutions, linear range 5.0 μM–10.0 mM and sensitivity of 22.8 μA mM^{-1} cm^{-2} (*112*). The authors found that the graphene oxide layer enhanced the sensor sensitivity compared to the case in which this layer is not present.

Santafé et al. (*113*) studied the effect of 1-ethyl-3-methylimidazolium ethylsulfate [C$_2$mim][EtSO$_4$] on copper-catalyzed luminol chemiluminescence (CL). A clear difference in the light emission was observed that was ascribed to a strong interaction between Cu^{2+} and the imidazolium ring of the IL. Interesting effects of [C$_2$mim][EtSO$_4$] on glucose oxidase activity were also noticed, and this enhancement was employed to perform sensitive chemiluminescent glucose detection (LOD = 4 μM) at pH 8.0 (*113*).

ILs have been used in the detection of volatile, biologically relevant compounds such as NO. In one example, 1-hexyl-3-methylimidazolium hexafluorophosphate has been used in combination with a double chain surfactant to replace Nafion® as an antifouling layer on top of electrodes modified with poly(eosin-b). The results showed that the IL composite modified electrode exhibited excellent anti-interference behavior against nitrite, for example, and a wide linear relationship over NO concentrations ranging from 36 nM to 0.13 mM (*53*).

Before concluding this section, it is noting that electrochemical sensors in the literature often rely on the use of stable and reliable standard reference electrodes, e.g., Ag/AgCl, with an inner filling solution, typically KCl. However, ideally, the reference electrodes should be mass produced, e.g., prepared from a scalable automatic process like screen printing, and they should be maintenance free, or at least require minimal maintenance. These demands are driving the increasing trend toward solid-state functional components (*114*). As novel designs for reference electrodes that, for example, do not rely on an inner-filling solution, are much needed, IL related developments emerging from materials science research may offer advantages. For instance, Cicmil et al. (*115,116*) reported on the use of ILs in polyvinyl chloride (PVC) matrices for the preparation of disposable reference electrodes in which the partitioning of the ions into the liquid phase defines the interfacial potential. After comparing several ILs, the authors found that reference electrodes prepared with 1-ethyl-3-methylimidazolium bis(trifluoromethanesulfonyl) imide [C$_2$mim][NTf$_2$] were least sensitive to changes in the concentration of common alkali metal chlorides. The authors successfully employed these reference electrodes for the potentiometric measurement of Pb^{2+} solutions, cyclic voltammetry of a solution-phase redox probe, and impedance spectroscopy of a polymer membrane. Results comparable to standard reference electrodes have been obtained with hydrophobic ionic liquids, such as 1-methy-3-octylimidazolium bis-(trifluoromethylsulfonyl)imide, which was jellified and saturated with AgCl (*117,118*). The electrodes suffered from component leaching and signal deviations (in the mV range) due, for example, to phthalate ions or chloride interference at concentrations greater than 0.1 M (*117,118*).

13.09.2.2.2 Ionic Liquids for Sensing Ions

There are various motivations for developing novel membrane materials in ion-selective electrodes. These include the need for biocompatibility, elimination of plasticizers, minimize leaching, miniaturization, increasing the selectivity and stability, and improving detection limits (*119*). An attractive advantage of ILs is the ability to use them to tailor or tune the properties of a material, such as the solvation environment that determines ion extraction and complexation equilibria within a membrane (*85,119*). It may be that ILs will replace conventional ion exchangers (*119–122*), plasticizers, or even the ionophore in ISEs, but this area seems still in its infancy and only a few examples have been published in the literature (*119,120,123,124*).

When using ILs as plasticizers, the mechanical properties of the membranes formed have to be taken into consideration. For example, it was found that imidazolium-based ILs plasticize poly(methyl methacrylate) (PMMA) but not PVC, i.e., membranes plasticized with PVC, are found to be brittle and inductile (*120*). In addition, it should be noted that ILs influence the fluidity of the membrane, thus determining the diffusion coefficient of the ions and therefore the sensor response time and detection limits (*119*).

In addition, ILs are known to have larger dielectric constants, which in turn influences the ISEs' selectivity (*119*). For instance, Wardak (*124,125*) applied ILs as a solid contact in ISEs to study the effect of three different alkyl chains situated on the methylimidazolium cation, while keeping the anion constant (Cl^-). The author observed that the substituents in the imidazolium ring affected the limit of detection (LOD) of the sensors and the best results were obtained with 1-butyl-3-methylimidazolium. However, no explanation of the underlying reasons for this behavior was given. The optimized sensors could detect 40 ppm of lead in spiked tap, river, and waste water using the standard addition method, which was in good correlation with data obtained from anodic stripping voltammetry.

Beyond ion-selective electrodes, ILs may be employed as electrocatalyst for the detection of ionic species of clinical importance. For instance, a new iron(III)-containing ionic liquid $[(C_4H_9)_2\text{-bim}][FeCl_4]$ (Fe-IL, bim = benzimidazolium) was developed as an electrocatalyst for detection of nitrite and bromate (*126*), which are classified as carcinogens (*127,128*). A conductive carbon paste electrode (Fe-IL/CPE) comprising Fe-IL and carbon powder was fabricated, and the Fe-IL had the advantage of being both a binder and the electrocatalyst. The detection limit and the sensitivity were found to be 0.01 μM and 100.58 μA μM^{-1} for nitrite, and 0.01 μM and 83.11 μA μM^{-1} for bromate detection, respectively.

13.09.3 Recent Trends in Sensing with Conducting Polymers

13.09.3.1 Introducing Conducting Polymers

CPs are organic polymers with intrinsically high electrical conductivities. They have received ever-increasing attention since the seminal contribution of Heeger, MacDiarmid, and Shirakawa, who jointly received the Nobel prize for chemistry in 2000 (*129–132*). While they were initially investigated as substitutes for metals, their range of applications quickly expanded covering several research fields such as electrocatalysis, energy storage, and sensing (*133*). Today's conductive polymer workhorses are primarily derivatives of polypyrrole, polythiophene, polyaniline, and poly(3,4-ethylenedioxythiophene), see **Figure 3**.

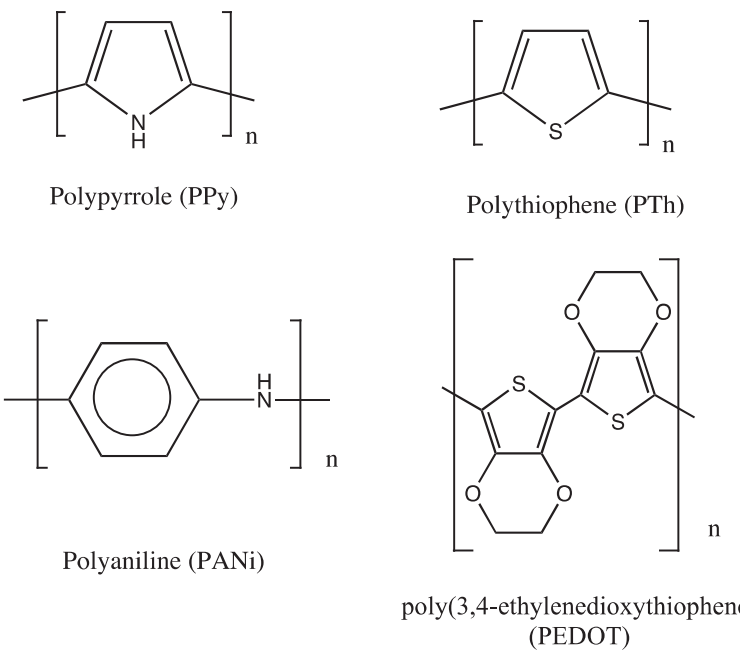

Figure 3 The most common CPs in the undoped form including polypyrrole (PPy), polythiophene (PTh), polyaniline (PANi), and poly(3,4-ethylenedioxythiophene) (PEDOT).

Next, we present a brief overview on conducting polymers with references available if the reader wishes to explore further. Some particularly important contributions are summarized.

Chujo (*134*) and Leclerc and Morin (*135*) focused their attention on the synthetic aspects of the preparation of CPs. A book containing several contributions that span from the fundamental aspects of CPs, e.g., mechanism of growth and electrochemical characterization, to their recent applications in sensing, in energy storage, and as artificial muscles is available by Cosnier and Karyakin (*136*). Wallace and coauthors (*137*) compiled a concise but detailed book that describes their wide range of applications and gives a brief insight into the preparation and characterization of the most common CPs employed in the literature, i.e., polypyrrole, polyaniline, and polythiophenes. Eftekhari (*138*) presents some recent methods to control the morphology of conducting polymers at the nanoscale. Skotheim and Reynolds (*139*) provide a detailed coverage of recent advances in the chemistry, physics, and materials science of conjugated and conducting organic polymers. Gerard et al. (*140*) presented a review that describes the salient features of conducting polymers and their wide applications in health care, food industries, and environmental monitoring. Lin et al. (*141*) published an overview of organic thin-film transistors as chemical and biological sensors, describing in detail the sensing mechanisms and the detection limits of these devices. Nambiar et al. (*142*) focused on the use of CP-based sensing devices as tools in clinical diagnosis and for assisting surgical interventions; e.g., electrochemical biosensors, tactile sensing 'skins,' and thermal sensors. Ates and Sarac (*143*) reported on the electrochemical deposition of conducting polymers on carbon substrates for biosensor preparation while Rozlosnik (*144*) focused on the use of PEDOT in biosensing.

Amongst the most popular CPs being investigated for sensing applications are PPy and PEDOT derivatives. PPy is known for its good mechanical properties, but this is counterbalanced by low ion accessibility due to its dense films, relatively low conductivity (10–50 S cm^{-1}), and chemical instability, for example, due to oxygen (*145*). PEDOT is the most popular CP among the polythiophene family. Compared to PPy, PEDOT has 10 times greater conductivity (300–500 S cm^{-1}), greater chemical and thermal stability, and higher optical transparency (*144–146*). The green emeraldine salt form of PANi has conductivity in the range 1–10 S cm^{-1}. Furthermore, PANi has the ability to form a broad range of nanostructures without the use of a template (*147*). A general feature of CPs is that they change their properties, such as conductivity or optical properties, depending on the doping state that has been used as transducing principle, i.e., when the analyte changes the doping state of the polymer. Another attractive feature of CPs in the preparation of disposable and low-cost sensors is their compatibility with inkjet printing (*148,149*) or electrospinning (*147*). In addition, polymer-based organic electronics based on CPs may open the way to the creation of inexpensive flexible devices and offer the possibility of integration of sensing/electronic devices with wearable fabrics (*150–152*).

In recent years, there have been considerable efforts to improve the chemophysical characteristics of CPs. Of particular interest has been the possibility of improving the mechanical, physical, and chemical properties of CPs by integrating ILs during their electropolymerization (*84,87,146,153–155*). For instance, control of the water content during the electropolymerization seems to affect the conductivity of the CP layers. This was observed during the electropolymerization of thiophene in an aqueous electrolyte, and it resulted in the formation of a nonconducting polymer film (*97,156*). In addition, the choice of IL cation/anion is important as it affects the stabilization of the radical produced during IL electrochemical oxidation and regulates the degree of electrostatic interaction between the anion and the polymer backbone (*83,97*). In addition, ILs may affect chemical doping of the polymer film, the polymer film thickness, and film morphology (*83*). For example, pyrrolidinium-based NTf_2-ILs led to polythiophene films that were smoother and denser than those produced using imidazolium-based NTf_2 ILs (*83,150*). While these differences were ascribed primarily to the different viscosities and conductivity of the ILs, effects arising from the cation during the electropolymerization cannot be totally excluded. In certain cases, ILs may affect the structuring of the polymer chains at the nanoscale, as demonstrated by Ahmad et al. (*146,150*), who showed that 1-ethyl-3-methylimidazolium bis(perfluoroethylsulfonyl)imide assisted fiber growth in PEDOT films. These nanostructures tend to shorten diffusion distance for ion transport, which affects the polymer charge/discharge capacities and rates (*157*) while also increasing electrocatalytic activity (*150*). Interestingly, co-deposition of PPy and PEDOT has been demonstrated in ILs (*145*). This particular study highlighted that co-deposition resulted in a more porous film due to entanglement and mismatch of PPy and PEDOT chains (*145*).

Finally, it is important to acknowledge some issues that may arise with CPs, such as concerns over thermal and chemical stability, the mechanical ruggedness, and tolerance to high-field electric fields of CPs (*73,142*), all of which may affect the performance of CP-based sensors. Recent research has focused on finding solutions to some of these issues, and the electrochemical growth of CPs in new media like ILs, as highlighted previously, has offered some improvements. In addition, while CPs are generally regarded as noncytotoxic to mammalian cells, there is still concern about their long-term impact, and therefore there is considerable interest in producing new types of biodegradable CPs (*73*).

13.09.3.2 Customization of Conducting Polymers for Biomedical Applications

13.09.3.2.1 Conducting Polymers in Biosensors

CPs have been successfully used in the preparation of biosensors in order to entrap enzymes *in situ*; however, in certain cases the high enzyme loading has proven to impede the electropolymerization of the CP (*158*). It should also be noted that, if hydrogen peroxide is developed as a by-product of the oxidase enzymatic substrate conversion during the sensor activity, this compound can cause the overoxidation of the CP and limit the lifetime of the sensor (*12*). Therefore, the sensor requires careful designing in order to minimize H_2O_2 formation.

A few examples of the use of CPs in the fabrication of biosensors are detailed next.

Two polythiophene derivatives, poly(4,7-di(2,3)-dihydrothienol[3,4-b][1,4]dioxin-5-yl[1,2,5]thiadiazole) and poly(4,7-di(2,3)-dihydrothienol[3,4-b][1,4]dioxin-5-yl-2,1,3-benzoselenadiazole), have been employed in order to increase the stability of the adsorbed GO_x enzyme thanks to enhanced π–π stacking and electrostatic interactions (*159*). The modified electrodes were capable of detecting glucose in real human serum samples, although these were diluted with buffer solutions to coincide with the limited sensor dynamic range, that is, 0.05–1.0 mM (*159*). In addition, the immobilization of GO_x on top of the CP layers with glutaraldehyde seems to be a serious limitation as this compound may cause the denaturation of enzymes.

Rahman et al. (*51*) showed that poly-5,2′-5′,2″-terthiophene-3-carboxylic acid (TTCA) electrochemically grown at gold electrodes can be used to complex Mn(II) through the carboxylic groups of the CP. The resulting film was used as biocatalyst for the oxidation of bilirubin and, with the addition of an anti-interference layer, the biosensor could detect bilirubin in a human serum sample, although this was diluted with a buffer (*51*). The bilirubin content was measured to be 5.2 ± 0.7 μM, which is reasonably consistent with the result obtained from a spectrophotometric method (4.9 ± 0.2 μM). TTCA polymer was also used for the preparation of NO sensors. In fact, the polymer was electrochemically grown on platinum microelectrodes and the CP was covalently attached to cytochrome-*c* (*160*). After coating with Nafion®, the modified microelectrode showed a linear response for NO in the range 2.4–55 μM, allowing the detection of NO *in vivo* in rat brain tissue (*160*).

Polyaniline has been polymerized by the hydrogen peroxide produced enzymatically by GO_x in the presence of glucose (*161*). The gluconic acid, produced enzymatically, causes a pH drop that triggers the catalytic polymerization of aniline (*161*). Interestingly, in this manner, the physically adsorbed enzyme could be encapsulated within a polyaniline layer that limits the rate of leakage of the enzyme (*161*). Polyaniline nanoparticles and urease have been successfully incorporated onto a flexible substrate using inkjet printing in the preparation of urea sensors (*148*). The biosensor could measure urea in the range of 2–12 mM, but the data obtained for the urea content in 15 human serum samples showed a positive bias against a spectrophotometric assay. Polyaniline, thanks to its pH-dependent doping states, seems to be a popular material for the preparation of ammonia sensors that have been successfully applied in the monitoring of human breath samples. For instance, an amperometric sensor was created by electropolymerizing aniline onto gold nanoelectrodes (*162*). By increasing the concentration of ammonia, the current decreased due to de-doping of the conducting polymer. Tests with real breath samples correlated well with a laboratory standard colorimetric technique for ammonia detection with a discrepancy of 12%, possibly due to experimental differences in the sample handling (*162*).

Nanostructures based on CPs have received great attention in the literature (*138*) and have been applied to sensing. For example, poly(toluidine blue) nanowires, prepared from a template-directed electrochemical deposition, have been used to load and stabilize horseradish peroxidase (HRP) (*163*). The resulting sensor showed good linear response to H_2O_2 over a wide substrate concentration range, although the template deposition method can be cumbersome and may suffer from the potential leaking of the adsorbed enzyme. With regard to template-less polymerization, for instance, pyrrole has received much attention due to the possibility of producing nanostructures during its electrodeposition; fibrillar, rod, and worm-like structures can be prepared using carbonate or phosphate salt solutions (*164–168*). The mechanism behind the formation of the nanostructures is still controversial, but it has been hypothesized it may be due to the low density of the charge carriers during the polymer growth and alignment of PPy chains bridged by the phosphate or carbonate anions (*164,169*).

CPs may be tailored in order to introduce chemical functionalities into the polymer backbone, as this can provide anchoring sites for specific sensing tasks such as binding aptamers for the development of highly sensitive aptasensors. For instance, the extended π-conjugation along the backbone of poly(*m*-phenylenediamine) (PMPD) allows the physical adsorption of a dye-labeled thrombin aptamer onto the surface of PMPD rods (*170*). Indeed, the presence of these aptamers on the surface of the rods induced substantial quenching of the fluorescence dye, which was recovered only in the presence of thrombin, due to the formation of the quadruplex–thrombin complex. Luo et al. (*171*) covalently attached the immunoglobulin E (IgE) aptamer to the amino groups of the PANi backbone. Using this approach, it was possible to prepare a conductometric and label-free aptasensor for IgE that relates to cancer pathologies (*172*). The detection principle is based on the notion that the high surface-to-volume ratio of the nanostructures is markedly affected by minor perturbations of their electrical field induced upon binding of IgE (*173*).

13.09.3.2.2 Sensing Ions and Conducting Polymers

In solid-contact ISEs (SC-ISEs), the internal reference electrode and inner filling solutions can be replaced by solid materials (*114,174–178*). SC-ISEs are more convenient for remote monitoring than liquid-filled ISEs as they are more compatible with microfabrication technologies (*114,174–178*). While CPs have been extensively used as a solid contact material, it is important to note that the choice of the conducting polymer is imperative in the ISE's longevity as it will affect the stability over time and the LOD (*114,129,174–185*). In addition, the type of CP to be used as a solid contact can also depend on the ion analyte (*186*). Poly(3-octylthiophene) has been used as a solid contact due to its hydrophobicity as this improves membrane adhesion and limits water uptake (*177,187*). PANi was also used as SC layer in potassium-ISEs, which have been used for the detection of potassium in artificial serum, with a linear range between 10^{-5} and 10^{-1} M and no pH interference under physiological conditions (*188*).

While PANi, PPy, and PEDOT have been extensively investigated as solid contacts in ISEs, the possibility of improving SC-ISE performance using other CPs or by CPs nanostructuring seems to be relatively unexplored (*189*). For instance, polypyrrole microcapsules have previously been employed as solid contacts in calcium-ISEs (*190,191*). The authors claim that through this, they can control the electrolyte composition of the microcapsules, thus providing a means to fine-tune the LOD.

The use of neat CPs or CPs doped with selected ionophores as a sensing layer is an interesting approach. However, thus far, such sensors suffer from poor sensitivity and high LODs (*144,189,192,193*). PANi deposited on plastic substrates by means of ink-jet

printing was used to detect pH changes both potentiometrically and spectrophotometrically (*192*), but the selectivity factor hampered their use in real-sample scenarios (*192*). A stripping voltammetric sensor based on an overoxidized PPy film was developed for the detection of copper in human hair (*194*). The device had a sensitive range from 2 to 250 ng ml^{-1}, and experimental results were in agreement with results obtained from atomic absorption spectroscopy. This particular sensor could be regenerated by washing with EDTA solutions, without appreciable differences in response characteristics before and after the washing step. Finally, PEDOT drop-cast nanorods produced by interfacial polymerization on a glassy carbon electrode showed high electrocatalytic activity for nitrite oxidation (*195*). The amperometric sensor showed a linear response in the range 0.6–40 μM and a sensitivity of 22.8 μA mM^{-1}. However, the sensor was not tested with real samples.

A recent nice example of a CP-based sensor employed poly(9,9-bis(6′-benzimidazole)hexyl) fluorine-*alt*-1,4-phenylene. This is a water-soluble fluorescent polymer that has been used for the detection of phosphates in blood serum (*196*). The phenyl benzimidazole group of the polymer is able to selectively bind Fe(III), which in turns quenches approximately 97% of its fluorescence. However, phosphates restore more than 95% of the polymer fluorescence as they bind to the Fe(III). Because of the control of the polymer fluorescence exerted by Fe(III) and the phosphates, the authors were able to use the polymer to detect phosphates in blood serum samples. The sensor-determined levels of phosphate were in the range 4.24–4.37 mg dl^{-1}, which was in good agreement with the value of 4.46 mg dl^{-1} obtained by standard spectrometric and potentiometric assays employed in clinical practices (*196*).

13.09.4 Recent Developments in Nanomaterial-Based Sensors

13.09.4.1 Metal Nanoparticles

13.09.4.1.1 Introduction to Metal Nanoparticles

Metal nanoparticles (NPs) date back in time since their first applications in glass staining to create color-changing effects (*197*). Faraday gave the first scientific explanation of their optical properties, suggesting that the interaction of the light with the colloids is at the basis of their color. Nowadays, this behavior is understood as originating from localized surface plasmons that oscillate with a characteristic frequency which is sensitive to the changes in the local dielectric environment (*197*). In recent years, nanoparticles have been at the center of tremendous research attention, most notably through the work by Brust et al. (*198*), who developed an easy pathway to their chemical synthesis and stabilization. Chemical synthesis is still one of the best approaches for their preparation, although other methods such as evaporation under vacuum or laser ablation (*199*) have also proven effective. Nanoparticles have been prepared using different metals such as gold, silver, platinum, and palladium, with each metal imparting specific catalytic and optical properties (*200*,*201*). In NP chemical synthesis, the choice of ligands, the metal to reducing agent ratio, time, and temperature all play an important role in determining the morphological aspects and properties of the resulting NPs (*199*). While a detailed discussion is beyond the scope of this chapter, the reader can find valuable information in several excellent references, which are summarized here.

Kelly et al. (*202*) described how size, shape, and dielectric environment influence the optical properties of metal NPs; Narayanan and El-Sayed (*203*) described the use of NPs as electrocatalysts; and Murray (*204*) discussed the electrochemical properties of metal NPs and their incorporation in electrochemical devices. Schmid (*197*) edited a comprehensive book introducing the booming field of the 'nanoworld' and covering aspects of nanoparticles from their fundamental principles to their use in novel applications. Rotello (*205*), from a chemical standpoint, described the diverse structures and properties of nanoparticles, presenting also fundamental studies and pragmatic applications ranging from materials research to device fabrication. Nagarajan and Hatton (*206*) published a book covering recent advances in the synthesis, stabilization, passivation, and functionalization of nano-objects made from a wide range of materials, such as metals and metal oxides. Methods to control the number of functional groups and to attain aqueous dispersibility, the impact of stabilizers on SERS activity and ways to tune plasmon resonance via nanoparticle shapes were also presented.

An attractive advantage of nanoparticles is the possibility to tune the plasmon resonance in order to match a biological window of tissue transparency, so as to coincide with an emitter excitation or to match a laser source (*207*,*208*). For this reason, nanoparticles have been extensively used for analytical purposes, in particular as labeling components for biological compounds such as DNA, enzymes, and antibodies (*209*). Another useful property of metal NPs is that they quench fluorescence. For instance, fluorescent polymer conjugates coupled with gold nanoparticles have been prepared for sensing of proteins such as bovine serum albumin, β-galactosidase, or phosphatase (*210*). Indeed, the presence of proteins disrupts the NP–polymer interaction, producing distinct fluorescence response patterns that are characteristic of individual proteins at nanomolar concentration (*210*).

Synthetic methods to functionalize NPs have achieved a great level of control and sophistication such that NPs can be prepared with an innumerable number of different ligands and coatings, offering therefore enormous opportunities in tailoring specific properties for sensing applications. For instance, the problem of the electrochemical stability of the solid contact material in SC-ISEs is well documented, and CPs have been employed to tackle it, as discussed in the previous section (*211*). Nanoparticles may also have a role to play in solving this issue, thanks to their chemical stability and tunable properties, for example, through control of the ligands and the core materials used in their fabrication (*211*).

A core goal of nanotechnology is the ability to manipulate materials at the nanoscale. In this regard, control over the shape and alloy spatial distribution, at the nano- and microscale, that can be obtained through the use of nanoparticles is striking. In fact, it is possible to carve metal nanoparticles in an aqueous medium at room temperature (*212*,*213*) or to control their spatial network distribution by means of external stimuli in order to create tailored architectures (*214*,*215*). NPs may also offer advantages for the

customization of low-cost optical sensors integrated in Lab-On-A-Chip platforms (216), paper-based sensors and microfluidics, and in point-of-care devices (217–219).

13.09.4.1.2 Metal Nanoparticles for Biomedical Applications

The conjugation of DNA or aptamers with NPs has opened new routes in biosensing because it combines the selectivity and the affinity of these proteins with the advantageous spectroscopic properties of NPs (220). For instance, the shift in surface plasma resonance (SPR) upon the specific binding of the target analyte to the aptamer has been exploited for the detection of cocaine (221). Zhang et al. (222) developed a selective cocaine aptasensor where two sequences of cocaine aptamer stabilized the Au-NPs upon salt addition if no cocaine was present. In the presence of cocaine, aggregation occurred and the SPR of Au-NPs shifts, producing a color change from red to blue. Willner et al. (223) worked on the use of aptamers in order to create smart surfaces, which respond to a desired target analyte. For instance, a cocaine aptasensor was developed using two anti-cocaine aptamer subunits; one subunit was assembled on a gold support, acting as an electrode or an SPR-active surface, and the second aptamer subunit was labeled with Pt-NPs or Au-NPs. The addition of cocaine resulted in the formation of supramolecular complexes between the NPs-labeled aptamer subunits and cocaine on the metallic surface. Depending on the type of nanoparticles, cocaine could be detected from the reduction current of H_2O_2 electrocatalyzed by the Pt-NPs or from the reflectance changes stimulated by the electronic coupling between the localized plasmon of the Au-NPs and the surface plasmon wave. The detection limit for cocaine was at best 1 μM. A long response time, ~30 min, and the need to control the ionic strength of the solution seemed to be the major hurdles for this sensor configuration (223). Visual detection of cocaine was performed using a DNA modified linear polyacrylamide polymer, which was crosslinked with a cocaine aptamer and loaded with Au-NPs. In presence of cocaine, the hydrogel dissolves and Au-NPs are released in solution, turning its color from colorless to red and thus allowing its detection (224).

Au-NPs have been largely employed as a colorimetric transducer due to their attractive optical properties such as high extinction coefficient and marked color change accompanying aggregation (225,226). For example, a colorimetric assay for the detection of cerebral glucose was reported by coupling Au-NPs modified with adsorbed single-stranded DNA (ssDNA) (227). The hydroxyl radicals provided by the reaction between the enzymatically produced H_2O_2 and Fe^{2+}, both added to the solution containing the NPs, caused the cleavage of the adsorbed ssDNA. The addition of sodium chloride caused aggregation and therefore a change in color from red to blue. Similarly, bare Au-NPs and cationic conjugated polyelectrolytes were employed for the detection of DNA, cocaine, and thrombin (228). Interestingly, the latter method provides a simple and rapid way to visually detect thrombin at a concentration as low as 10 nM.

In the field of immunosensors, Au-NPs have found application in the detection of cancer biomarkers (229). In fact, it has been shown that for the detection of CA15-3-antigen, a known breast cancer biomarker, the application of Au-NPs labeled with HRP and CA15-3-antibody enhanced the sensitivity and shortened the incubation time of a commercially available ELISA immunoassay from 30 to only 5 min (230). Stevens et al. (231) developed a colorimetric prostate specific antigen (PSA) nanosensor, using gold nanostars. An antibody was tagged to GO_x that in the presence of PSA caused the formation of the antibody–antigen-labeled antibody complex. In the presence of glucose and silver ions (both added to the solution), GO_x converted glucose to gluconolactone and H_2O_2, which then reduced silver ions around the gold nanostars (231). When the concentration of GO_x was low, i.e., proportionally to antigen concentration, a homogenous silver coating on the nanostars was observed causing a large blue-shift of the SPR of the nanostar (231). This resulted in an exceptional detection limit of 40 fM for the PSA cancer biomarker in whole blood serum.

Khlebtsov et al. (232) introduced a multiplexed colorimetric dot immunoassay on a nitrocellulose membrane strip for simultaneous detection of rabbit anti-chicken, anti-rat, and anti-mouse antibodies. Ag nanocube, Ag/Au alloy nanoparticle, and Ag/Au nanocage probes, **Figure 4**, were labeled with chicken, rat, and mouse immune-gamma globulin (IgG) in order to generate spots of yellow, red, and blue colors, respectively (232). Upon spiking known concentrations of the target analytes on top of the nitrocellulose membrane, the latter was exposed to a solution containing a mixture of the three nanoprobes and the analyte–probe pair specifically formed. The resulting stained the nitrocellulose membrane as shown in **Figure 4** from reference (232). Using this approach, concentrations as low as 20 fM of the target analyte could be detected by the human eye.

The NPs developed by Strömberg et al. (233) were used in an optode for the detection of ammonia in porcine skeletal muscle tissue. The signal was analyzed by image processing and an LOD of 2 nM was achieved without any other ionic interference from the sample. The sensor was based on a hydrogel loaded with Au-NPs, 2-(dodecyloxy)benzonitrile, merocyanine, and nonactin, which acts as the ammonium carrier (233). As the porcine skeletal muscle tissue was sandwiched between a silicone sheet and the gas permeable membrane, the ammonia released was protonated to ammonium within the hydrogel, which in turns changed the fluorescence of the nanoparticles (233). This device may be implemented in breath diagnostic devices for patients with metabolic disorders or in artificial nose and tongue devices. Detection of Ca^{2+} in animal and human serum samples was achieved by functionalizing the nanoparticles with calsequestrin, which is a protein of the sarcoplasmatic reticulum able to reversibly bind calcium (62). The electrostatic interaction between calcium and calsequestrin caused nanoparticle aggregation, which in turn produced a visible color change from red to purple (62). Zhang et al. (234) developed a colorimetric assay for iodine using a nanoalloy particle of a copper core surrounded by a gold shell. The iodine caused a color change from purple to red, which was proposed to be due to a transformation of the interconnected, irregularly shaped nanoparticles to the single, separated, and nearly spherical ones. The sensor was able to monitor iodine concentrations (6 μM), with interferences from other ions occurring only when their concentrations were in the mM range. However, the color change was relatively slow, taking around 20 min (234).

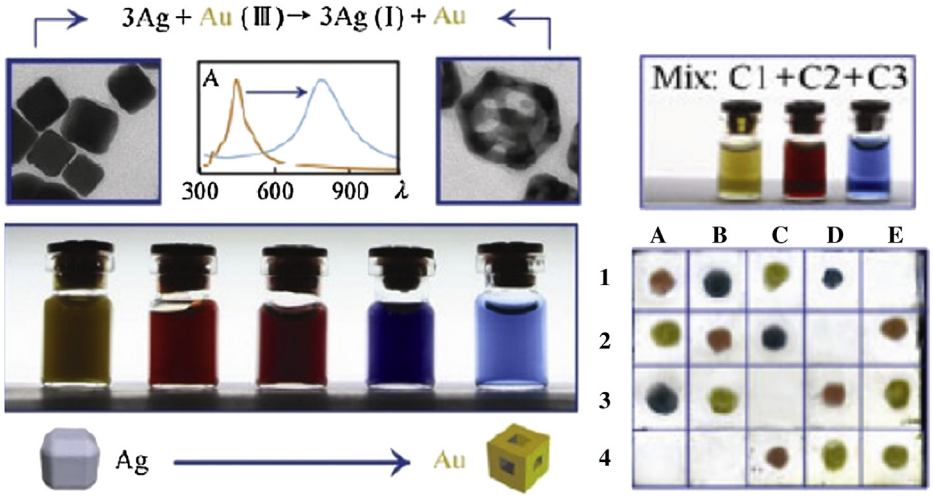

Figure 4 On the left side, TEM images of Ag cubes and of Au/Ag alloy nanocages together with pictures of vials containing their colloidal suspensions. On the right side, results obtained with the multiplexed dot immunoassay for the three target analytes on the nitrocellulose membrane. Reprinted with permission from reference Panfilova, E.; Shirokov, A.; Khlebtsov, B.; Matora, L.; Khlebtsov, N. *Nano Res.* **2012**, *5*, 124–134.

13.09.4.2 Carbon Nanotubes and Graphene

13.09.4.2.1 Carbon Nanotubes and Graphene – An Overview

Carbon nanotubes (CNTs) exist mainly in two forms, single- and multiwall, respectively termed SW-CNTs and MW-CNT. SW-CNTs can be considered as a long, wrapped graphene sheet consisting of two separate regions (side and end cap) with very different physical and chemical properties (*235*,*236*). For instance, certain studies imply that the tips of CNTs are more reactive than the cylindrical parts (*235*). MW-CNTs consist of concentric SW-CNTs of different diameter, in which the shells of carbon are closely separated (*235*). The lengths of CNTs play an important role in determining the electrical, optical, and mechanical properties (*236*).

CNTs have attracted great attention not only for their electrical properties but also because they seem to promote electron transfers to and from immobilized biomolecules, which is appealing for preparing biosensors (*235*,*237*). For example, enzymes have been immobilized on CNTs (*238*), although it has also been reported that the activity of enzymes may decrease considerably after their adsorption onto surfaces modified with CNTs (*239*). In this regard, the use of appropriate dispersant agents, e.g., ILs, may avoid the denaturation issue (*239*). It is perhaps worth noting that the CNTs' electrocatalytic properties are somewhat controversial. In fact, it has been suggested that it is the presence of metal impurities introduced during the preparation of CNTs, rather than the CNTs themselves, that provides the basis of the electrocatalytic behavior (*209*,*240*,*241*). In addition, there is still not unanimous agreement regarding the cytotoxicity of CNTs, although some authors support that functionalization of CNTs can control it (*240*,*241*). Finally, an important aspect to consider is the relatively high cost of producing and purifying CNTs (although this is decreasing over time), which may in some way explain the delay in their uptake by the industry (*235*,*240*).

Graphene is a unique material in which carbon atoms are arranged in a regular hexagonal pattern similar to graphite but in a one-atom thick sheet (*16*). It is a zero band gap semiconductor having conductivity akin to metals, which, in the opinion of some researchers, could provide the basis of materials with exceptional electrocatalytic abilities (*16*). Large-scale patterned growth of graphene is still problematic but progress is happening (*242*). For example, electrolytic exfoliation is particularly promising for producing graphene nanosheets in aqueous solution at low cost (*149*).

13.09.4.2.2 Applications of Carbon Nanotubes and Graphene in Biomedical Sensing

Carbon nanomaterials are particular suitable for use in biosensors due to their high surface/volume ratios and the possibility of immobilizing target molecules, e.g., bioreceptors, with high density. Thanks to their high conductivity and large surface-to-volume ratio, small changes on the conformation or displacement of the immobilized bioreceptors can be detected (*243*,*244*). This transduction mechanism has been reported in field-effect transistors (FET) (*2*,*69*,*245*,*246*) and may provide the basis of future devices like sensor-based bioelectronic noses and tongues (*114*,*236*,*247*), although, at present, the response patterns obtained by these devices are not stable over time (*2*). This is a serious limitation in bioelectronic tongues and noses, although their potential to extract complex information from the sensor array seems very powerful (*2*).

Dextran-modified, single-walled CNTs were employed as glucose biosensors in an FET configuration (*248*). In this sensor, concanavalin A, which was bound to the dextran layer, was displaced in the presence of glucose, producing a change in conductance (*248*). An et al. (*249*) reported an FET for the detection of thrombin using aptamer-modified, single-walled CNTs. The sensor had a linear sensitivity in the thrombin physiological range, i.e., from 70 pM to 70 nM. FETs based on carbon nanomaterials also have been reported to be responsive to pH (*250*) and sodium (*251*,*252*). For instance, sodium levels in the range from 1 nM to 1 mM were detected in serum samples. The operating mechanism is not fully understood, but it was suggested that the sodium ions bind

to the carboxylic groups on the graphene layer and the change of the sodium concentration modulates the current into the transistor (252). However, no tests with real body fluids were reported, which raises questions about their use in real scenarios.

Building precise sub-micrometer scaled scaffoldings and networks is important in order to impart certain functions to the sensing interface. Rusling et al. (253) employed SW-CNTs forests for the electrochemiluminescent detection of interleukin-6 (IL-6) and PSA, two cancer biomarker proteins. A charge-coupled device (CCD) camera was then used for the detection of the light generated by the silica NPs labeled with a ruthenium dye and the specific antibody, achieving detection limits of 1 pg ml^{-1} for PSA and 0.25 pg ml^{-1} for IL-6 (254,255). CNTs forests allow ample space between the pillars, but their preparation can be cumbersome (235,256). In this sense, a novel bucky-paper material prepared by Lard et al. (256) seems promising as it shows high surface adhesion and tunable electrical conductivity while maintaining separation of the individual tubes (256). The key material is a polymer with lamellar crystal structure. The polymer is perpendicular to the tubes and its size tunes the porosity, surface roughness, and conductivity of the bucky-paper (256).

Graphene offers excellent electron transfer properties, and this can play a key role in the performance of sensors (257). For example, ssDNA segments physically adsorbed on graphene quantum dots (GQDs) were reported for the detection of thrombin (258). The specific binding of the ssDNA with the target analyte generated an electron transfer between the electroactive species $[Fe(CN)_6]^{3-/4-}$ and the GQDs modified electrode, which would have otherwise been blocked by the adsorbed ssDNA. Nitrite sensors were also reported, based on immobilization of hemoglobin on graphene sheets functionalized with tetrasodium 1,3,6,8-pyrenetetrasulfonic acid (259), which binds to the positive domains of myoglobin (260). Graphene enhanced the electron transfer kinetics of the protein, and nitrite levels could be amperometrically quantified in the range of 0.01–2.5 mM. However, it was found that the signal was pH dependent, which limits the practical applicability of the sensor. Graphene may also improve the solid contact characteristics of ion-selective electrodes due to its exceptional electrochemical properties and hydrophobicity. In this regard, MW-CNTs employed as the solid contact in ion-selective electrodes have been reported to result in improved stability compared to CPs (261).

Graphene-based fluorescence quenching has been employed as the basis of several sensors. For instance, potassium was detected by immobilizing a DNAzyme (deoxyribozymes) on graphene and then intercalating a commercial fluorophore within the DNA structure (262,263). It was found that the fluorescence emission was quenched by the graphene layer, but the addition of Cu(II) ions generated a fluorescence signal proportional to the metal concentration in the range 2–250 nM (263).

13.09.4.3 Nanocomposites

13.09.4.3.1 Introduction and Properties of Nanocomposites

Nanocomposites are formed by combining nanoscaled-materials in order to obtain synergetic effects (264,265), such as improvements in the sensitivity and LOD of sensors, and to limit biofouling (240). Nanocomposites have been also investigated as a means to create a suitable microenvironment for the stabilization of biomolecules (266). In this respect, the combination of ILs and nanoparticles appears to present particular promise (83,267). CPs loaded with NPs have also proven effective in enhancing the electron transfer between entrapped enzymes and the electrode (209). In SC-ISEs, the ion-to-electron transduction may result either from a Faradic redox process or from a double-layer charging process (268,269). In the case of a capacitive contribution, the use of nanocomposite as solid contact may be beneficial in order to increase the surface area and therefore the overall capacitance, which in turns has proven to improve the sensor stability (268). From a commercial perspective, the possibility of preparing nanocomposites at a low cost and the feasibility of using these materials in common industrial processes will be important. In this regard, it is worth remembering that graphene and PEDOT can be printed together using ink-jet printing (149).

13.09.4.3.2 Tailoring Nanocomposites for Biomedical Applications

Nanomaterials have been used in a combined manner in order to improve the stability of enzymes (270–272). For example, platinum NPs and CNTs were used to modify glassy carbon electrodes in order to improve the deposition of oxidase-enzymes (271). The glucose oxidase-based biosensor built using these two materials showed a linear response up to 10 mM glucose, with a detection limit of 250 nM and a response time of 5 s, but it was not tested with real samples. Wu et al. (273) prepared multi-functional microgel particles for optically sensing glucose and simultaneous self-regulation of insulin. This was achieved by copolymerization of a gel layer of 2-(dimethylamino)ethyl acrylate with 4-vinylphenylboronic acid onto Ag nanoparticle. The microgel layer swells as a function of glucose concentration resulting in a change of the local refractive index around the inorganic core and a marked decrease of the photoluminescence intensity of the Ag cores, which provided means to monitor the glucose concentration in solution. At the same time, the swelling of the microgel particles, which depends on the glucose concentration, was used to regulate the release of the insulin loaded within the particles, as shown in **Figure 5** from Ref. (273).

Serafin et al. (274) used a 1-butyl-3-methylimidazolium hexafluorophosphate IL in order to solubilize alcohol oxidase and 3,4-ethylenedioxylthiophene (EDOT). The polymerization of the EDOT on carbon screen printed electrodes (SPEs) was modified with gold nanoparticles, which resulted in the entrapment of the enzyme (274). The measured current for ethanol was 30% larger in cases where SPEs were modified with NPs. The sensor showed a linear range between 5 and 100 μM and a detection limit of 2 μM. Mixtures of colloidal gold modified graphite powder with a solid RTIL, *n*-octyl-pyridinium hexafluorophosphate, were combined with glucose oxidase to prepare paste electrodes (89,275,276). The proposed biosensor responded to glucose linearly over concentrations ranging from 5.0 μM to 2.6 mM, with a fast response (10 s), and the lifetime was reported to be over 2 months (275).

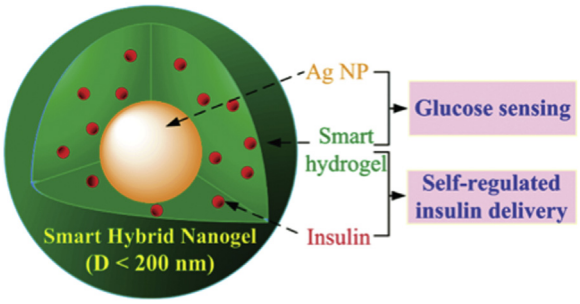

Figure 5 Schematic illustration of smart hybrid nanogels that integrate optical glucose detection and self-regulated insulin delivery at physiological pH into a single nano-object. Reprinted (adapted) with permission from Wu, W.; Mitra, N.; Yan, E. C. Y.; Zhou, S. *ACS Nano* **2010**, *4*, 4831–4839. Copyright (2010) American Chemical Society.

The effects of electroactive interferents, such as ascorbic acid and uric acid, were significantly reduced using a Nafion® coating, and the electrodes were used to analyze blood serum samples with good correlation with HPLC results, i.e., relative errors $< \pm 5\%$. These results are interesting as perhaps the graphite/ILs composite could be employed in ink formulations for the preparation of disposable glucose sensors.

Chitosan, which is a linear hydrophilic polysaccharide obtained by deacetylation of natural chitin, is attractive because of its biocompatibility, bioavailability, nontoxicity, and film-forming ability (*101*,*277*). It is pH sensitive and at pH values below its pK_a, i.e., pH < 4.5, it exists as a water-soluble cationic polyelectrolyte, while at higher pH, i.e., $\sim$7, it becomes neutral and insoluble (*101*,*277*). It has been largely used in nanocomposites for biosensing applications as it is thought to provide a good environment for enzyme stabilization (*101*,*277*).

Chitosan was electrochemically deposited at an electrode surface by lowering the local pH using a proton–consumer reaction (reduction of water or other oxidants in solution) (*101*,*277*). This deposition method provided good reproducibility of the film thickness and high surface area for the three-dimensional chitosan gel (*101*,*277*). During the biopolymer deposition, 1-butyl-3-methylimidazolium tetrafluoroborate [C_4mim][BF_4] and GO_x were also entrapped (*101*,*277*). The sensor thus prepared had a linear response for glucose in the 3 μM to 9 mM range. It was also able to detect glucose in serum samples, showing a good correlation to the measurements with standard commercial biochemical analyzers (*101*). A nanocomposite based on assembled layers of MW-CNTs, gold nanoparticles, 1-butyl-3-methylimidazolium tetrafluoroborate, and chitosan has been investigated as a means to immobilize cholesterol oxidase (*278*). The resulting sensor demonstrated good sensitivity with a dynamic linear range up to 5 mM, and cholesterol levels in serum samples were accurately measured using the standard addition method (*278*). NPs in chitosan–IL composite gels have also proven beneficial in biosensing (*279*). For instance, Au/Pt-NPs deposited within a chitosan/1-butyl-3-methylimidazolium chloride gel immobilized on a glassy carbon electrode coated with cholesterol oxidase using glutaraldehyde have been successfully used for cholesterol monitoring (*280*). The biosensor exhibited two wide linear ranges of responses to cholesterol, 0.05–6.2 mM and 6.2–11.2 mM. The sensitivity of the biosensor was 90.7 μA mM^{-1} cm^{-2}, the LOD was 10 μM of cholesterol, and the response time was less than 7 s. Levels of cholesterol in serum samples determined by the sensor agreed with those obtained by a standard clinical method, showing relative percentage errors smaller than 3% (*280*). However, the samples had to be pretreated with cholesterol esterase to convert fully the esterified cholesterol before the measurements were made.

CPs have been combined with other nanomaterials to enhance sensor performance, e.g., enzyme immobilization and sensitivity. Nanofibrous PEDOT has been deposited on glassy carbon electrodes by a micellar-assisted soft template approach using [C_4mim][BF_4] and sodium dodecyl sulfate (*281*). The IL works as a co-surfactant and as a dopant for PEDOT. Palladium nanoparticles were then deposited on the CP layer, followed by a potential-triggered deposition of GO_x and encapsulation using Nafion® (*281*). The sensor had a high sensitivity, 1.6 mA M^{-1} cm^{-2}, and was linear over a wide range of concentrations (0.5–30 mM). Besides, the sensor was able to detect glucose in diluted human serum samples, showing a small difference in relative percentage error (<3%) against values obtained with a standard reference method (*281*).

Poly-5,2′-5′,2″,terthiophene-3′-carboxylic acid was electropolymerized in the presence of MW-CNTs on gold electrodes, followed by chemical coupling of lactate dehydrogenase and its cofactor nicotinamide adenine dinucleotide, NAD^+, to the conductive polymer COOH groups. The sensor showed a linear response in the range from 5 to 90 μM and it retained 98% of its sensitivity after a period of 30 days (*39*). It should be noted, however, that commercial lactate test-strips can last up to 1 year. The sensor could detect lactate in human serum; however, samples had to be diluted 1000 times, and the standard addition method was employed, which is not a feasible practice in ready-to-use sensors.

Nonenzymatic sensors for the detection of molecules such as glucose, lactate, or ethanol is another important area of research due to the stability issues of enzymes when incorporated into biosensors. Certain conditions such as pH and temperature play a pivotal role in the stability of the enzyme, and therefore these sensors sometimes have a small operational window (*16*,*282*). Enzymatic approaches remain commercially unchallenged thanks to their reliability and low cost, i.e., few Euros per strip (http://www.novabiomedical.com/products/lactate-plus/). Research into enzyme-mimicking materials is typically focused on addressing significant issues such as fouling and selectivity (*16*). In this regard, combinations of ILs, CNTs, or graphene with metal nanomaterials seem a promising approach for the nonenzymatic detection of glucose (*16*,*209*,*283–287*).

Zhu et al. (*288*) studied the role of ILs in composites prepared by embedding Au-NPs in bucky-gels. The composite functioned as an electrocatalyst for the conversion of glucose. The authors gave evidence that imidazolium cations facilitate both the stability of sensor and the efficiency of NPs and CNTs in catalyzing glucose conversion, while non-imidazolium-based ILs work against the dispersion of CNTs and GNPs in the gel, reducing the detection sensitivity. It was also reported that the response to glucose can be improved by increasing the hydrophilicity of the anion. For example, ions such as sulfonate gave better results than BF_4^- and PF_6^-. Copper nanocubes deposited on vertically aligned MW-CNTs arrays were developed for the nonenzymatic detection of glucose, and the resulting sensors showed minimal interference from oxidizable interfering species such as fructose and ascorbic and uric acid (*289*). Results returned from human blood serum were close (within 5% relative error) to those obtained via standard tests. However, the requirement to add 0.1 M NaOH to the samples (dilution factor 1:1000) (*289*) may be a limiting factor in the preparation of ready-to-use sensors. Gold nanoparticles grown on CNTs were also reported for the electrocatalytic conversion of bilirubin, although the experiments were done in buffer solutions (*52*) rather than real samples, which limits the value of this output.

The use of magnetic nanomaterials offers certain advantages as magnetic separation is easy to implement and the composite can be easily collected for further analysis (*226,290,291*). Fe_3O_4 magnetic nanoparticles have been found to mimic the activity of peroxidases (*292*). This catalytic behavior, in combination with bioseparation and recycling, perhaps may be a plausible and exciting feature for the preparation of non-enzyme-based sensing strategies in which the sensing surface is newly generated each time, i.e., similarly to the hanging mercury drop technique. Tang et al. (*293*) introduced a microfluidic device for an immunoassay for simultaneous determination of carcinoembryonic (CEA) and alpha-fetoprotein (AFP) in biological fluids. The immunoassay was realized using anti-CEA and anti-AFP antibodies, immobilized on the Fe_3O_4 nanoparticle-coated graphene nanosheets. The magnetic composite allowed an easy separation from the biological specimen by application of a local magnetic field, avoiding the need of washing steps. In addition, the authors employed as antibody labels nanogold hollow microspheres, which provided higher loading capacity of the electrochemical active species (HRP-thionine and HRP-ferrocene) and larger surface coverage than bulk Au-NPs. The final immunosensors achieved an LOD equal to 1.0 pg ml^{-1} for both the target analytes.

We conclude this section reporting on a number of nanocomposites that have been used to modify electrode surface in order to improve sensor performance compared to bare surfaces (*294–298*). For example, simultaneous detection of NO_2^-, dopamine, and ascorbic acid was achieved using a nanostructured glassy carbon electrode modified with a graphene/MW-CTNs mixture dispersed in β-cyclodextrin and cyclodextrin prepolymer (*299*). As cyclodextrin exhibits different interactions with the three molecules, it was possible to differentiate them using differential pulse voltammetry (*299*). A linear range from 1.65 μM to 6.75 mM was achieved for NO_2^- and the sensor was successfully applied to the analysis of diluted urine samples spiked with the analyte of interest (*299*). Nanostructured polyaniline has been chemically synthesized using graphene oxide nanosheets as a polymerization template for adapting the surface of glassy carbon electrodes (*300*). Using this approach, it was possible to simultaneously differentiate between ascorbic acid, dopamine, and uric acid. NiO nanoparticles have been used as seeds for the polymerization of pyrrole, which was triggered by addition of $HAuCl_4$ after monomer adsorption on the NiO core. The nanocomposite worked as an electrocatalyst for the oxidation of biothiols, with the polypyrrole layer improving the composite adhesion to the electrode surface (*301*). Sensors developed using this method showed a linear response in the range from 0.35 to 9 μM for the detection of cysteine in saliva using the standard additions method, with almost no interference from other biological thiols like homocysteine and glutathione reported.

13.09.5 Ionogels: Diverse Materials for Sensing Platforms

13.09.5.1 Introduction to Ionogels

Ionogels are polymer gels in which an ionic liquid is integrated into the polymeric network. In these materials, the IL can often retain its specific properties within the polymer/gel environment. The employment of ILs as a replacement for water in gel-based polymers has led to the emergence of ionogels as a relatively new subclass of materials. To date, ionogels have been the subject of reviews detailing their preparation and applications in sensor science (*95,302*). The ionogel template is an ideal matrix as the properties of the IL is hybridized within those of the polymer component, combining the favorable characteristics of both independent phases in one material. An excellent review by Bideau et al. (*303*) discusses ionogels, in which the properties of the ILs are hybridized with those of various components. These may be organic (low–molecular weight gelator, polymer), inorganic (e.g., carbon nanotubes, silica, etc.), or organic–inorganic (e.g., polymer and inorganic fillers) as shown in **Figure 6**. Another approach for the preparation of ionogels is to use ILs in which the cation or the anion is polymerized, e.g., via vinyl groups. These ionogels are normally denoted as poly-ILs (PILs). This approach can be particularly effective in reducing the leaching of IL components into a sample (*304*).

The use of ionogels in electrochemical sensors and biosensors is an ever-growing field. An intrinsic advantage of ionogels compared to redox polymers is that their ion conductivity is decoupled from segmental motion, i.e., movement of polymer branches, providing high conductivity even below their glass transition temperature (*305*). As discussed in Section 13.09.2, in certain cases, ILs may exhibit favorable biocompatibility behavior, and stabilize biomolecules and enzymes, leading to enhanced sensor stability and shelf-life. Some examples are based on the immobilization of enzyme-IL systems with hyaluronic acid (*306*) or Nafion® (*307*). Ionogels may also assist in the preparation of stable conductive-textile yarns, maximizing contact surface and improving skin adhesion during sweating (*32,34,308*). This is an attractive proposition for the field of wearable textile biosensors. These materials should be capable of retaining the favorable properties of the base IL in a solid, semi-solid gel-like structure (*91*).

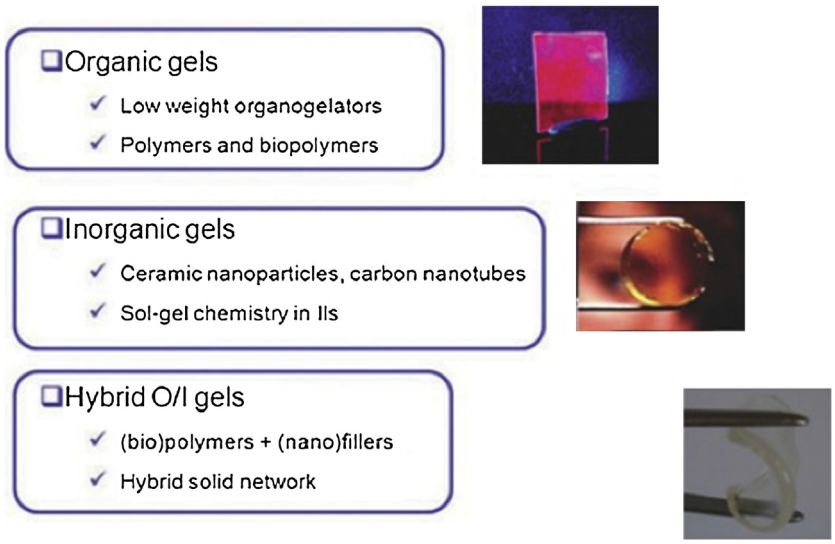

Figure 6 Types of ionogels synthesized as outlined by Bideau et al. Reproduced by permission of The Royal Society of Chemistry; Le Bideau, J.; Viau, L.; Vioux, A. *Chem. Soc. Rev.* **2011**.

13.09.5.2 Biomedical Applications of Ionogels

Perhaps the most common use of ionogels is to provide a suitable solid-state matrix for a stable encapsulation of nanostructured materials such as proteins and enzymes (*86,235,265*). For instance, PILs have been used for the electrochemical sensing of glucose. In fact, hydrophilic microparticles were prepared by emulsion polymerization of 1-vinyl-3-ethylimidazolium bromide in the presence of a cross-linker and GO_x (*309*). This method allowed the entrapment of the enzyme within the microparticles, which were then immobilized at the electrode interface (*309*). Using amperometry, glucose levels in serum human sample were validated, and the sensor showed storage stability up to 150 days when stored in frozen PBS at −4 °C (*310*). A polyethylenimine functionalized IL (PFIL) was successfully used as a matrix in aqueous solution to synthesize Au-NPs (about 2.4 nm) and simultaneously stabilize MW-CNTs (*311*). The nanocomposite (Au-NPs/MWCNTs/PFILs) once deposited onto glassy carbon electrodes could successfully 'wire' the glucose oxidase, which was physisorbed onto the nanocomposite. The sensor response was linear in glucose buffer solutions ranging from 2 to 12 mM, which is suitable for its practical application in determining blood sugar, although this was not demonstrated with the analysis of real samples. Similarly, graphene sheets were stabilized by a mixture of poly(vinyl-pyrrolidone) and PFILs, providing direct 'wiring' of GO_x, and they were successfully used in the sensing of glucose in aqueous solution (*312*). In another interesting example, methyl-imidazolium moieties were grafted on MW-CNTs in order to confine redox-active ferricyanide thanks to the strong electrostatic interactions (*313*). The nanocomposite was then coated with GO_x (through crosslinking with glutaraldehyde) and developed as a glucose sensor (*313*). Fonseca et al. (*314*) explored the application of new biocompatible materials by developing colorimetric glucose sensor strips in possible application of a new class of fully biocompatible ionogels. Imidazolium-based ILs paired with a gelling agent (gelatin type A) formed an ionogel, defined by the authors as Ion Jelly®, which provided a stable environment for the GO_x enzyme for up to 2 weeks of storage with 30% loss of stability (*314*). By incorporating GO_x, HRP, and the chromogenic dye precursors into the Ion Jelly® (in which IL was $[C_2mim][EtSO_4]$), the authors realized a colorimetric glucose sensing strip. This work is surely exciting; however, the accuracy of the colorimetric assay in determining the glucose level and the short shelf-life of such sensor (limited by the stability of the enzyme in the Ion Jelly®) seem to be two major hurdles in the system.

In recent years, developments in the field of organic electronics have led to novel approaches for producing flexible electronics using organic semiconductors (*315*). Among others CPs, PEDOT:PSS can be patterned on a wide variety of substrates such as glass, flexible plastic, and textiles, opening the way for the development of wearable biosensors. Such biosensors can be incorporated into fabrics such as T-shirts, sweat bands, or shorts, allowing for real-time measurements of the target analyte. In this respect, Khodagholy et al. (*316*) used a PEDOT:PSS OECT in which a pNIMAm/$[C_2mim][EtSO_4]$ ionogel was integrated as a solid-state electrolyte for the detection of lactate in the sweat physiological range (between 9 and 23 mM). As proof of concept, the authors demonstrated the use of OECTs in an array with a 'tattoo-like' format using a flexible substrate, i.e., parylene, as shown in **Figure 7**.

Regarding wearable sensors, ionogels may offer a simple route to generating simple colorimetric devices. For instance, Curto et al. (*317*) developed a colorimetric, wearable, microfluidic barcode for the real-time monitoring of pH in sweat, as shown in **Figure 8** (*318*). The barcode contains ionogels that are doped with several pH chromogenic dyes (having different pK_a) such that the device is capable of monitoring the pH in the range 4.5–7.5. The authors reported that the pNIPAAm/$[P_{6,6,6,14}][dca]$ ionogel provides a convenient matrix to immobilize the pH responsive dyes, as it reduces leaching of the dyes through electrostatic interactions within the IL. The device was integrated into a commercially available plaster, and was successfully used for measuring the pH of an athlete during a 50-min training session.

Bucky-gels, which are a mixture of carbon nanotubes (or graphene) and ionic liquids, have received considerable attention as a novel material for generating interesting sensing configurations (*319*). For example, an MW-CNT and 1-octyl-3-methylimidazolium

Figure 7 Concept of a flexible and conformal OECT/ionogel array worn on the forearm. Figure adapted from reference Khodagholy, D.; Curto, V. F.; Fraser, K. J.; Gurfinkel, M.; Byrne, R.; Diamond, D.; Malliaras, G. G.; Benito-Lopez, F.; Owens, R. M. *J. Mater. Chem.* **2012**, *22*, 4440–4443.

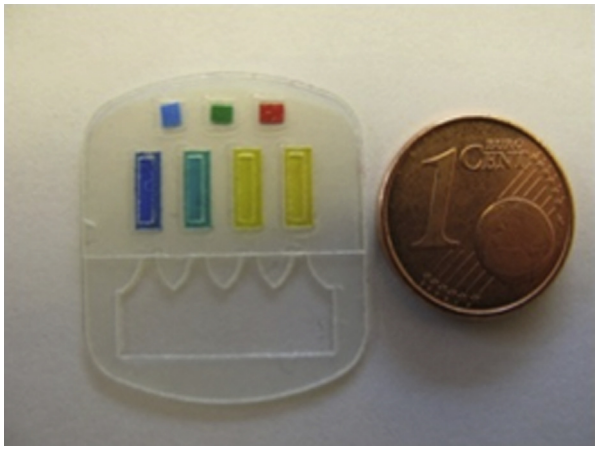

Figure 8 Flexible and wearable microfluidic barcode for real-time pH sweat analysis through the use of four pH sensitive phosphonium-based ionogels. Figure adapted from reference Curto, V. F.; Fay, C.; Coyle, S.; Byrne, R.; Diamond, D.; Benito-Lopez, F. Wearable Microfluidic pH Sweat Sensing Device Based on Colorimetric Imaging Techniques. In *The 15th International Conference on Miniaturized Systems for Chemistry and Life Sciences, μTAS 2011 (MicroTAS) Conference, Seattle, USA*, 2011.

hexafluorophosphate bucky-gel was decorated with ternary alloy nanoparticles based on Pt, Ru, and Ni (*320*). The sensor was applied to alcohol detection in aqueous solutions up to a concentration of 38 mM. Graphene mixed with 1-butyl-3methyl imidazolium hexafluorophosphate has been used in the fabrication of gels for the detection of NO in aqueous solutions (*321*). The sensor exhibited a fast response of less than 4 s, and a low detection limit of 16 nM, which is superior to that of NO sensing platforms based on carbon nanotubes and gold nanoparticles (*321*).

Ionogels represent an interesting approach also for the detection of ions and metal oxides by voltammetric methods such as stripping voltammetry (*322*), thanks to their solvation properties (*323*). For example, Wan et al. (*319*) incorporated thiols to improve the stability of bucky-gels on carbon electrodes and then used the modified electrodes to detect lead ions by means of stripping voltammetry. The authors reported the detection of lead at the femtomolar level and successfully measured lead content in lake water. Ionogels have been reported to provide a stable double layer capacitance and therefore overall stable sensor response in solid contact electrodes (*124*). The possibility of tuning the characteristics of an ionogel by varying the IL is an attractive proposition. For example, this has been used to control the hydrophobicity of ionogels and therefore the degree of swelling, which is critical for the realization of polymer actuators. It should be noted that hydrogels are not effective as materials for solid contact electrodes because of their natural tendency to absorb water (*324*). In contrast, using ionogels rather than hydrogels as the solid contact material in ISEs can reduce this problem, and this may improve the long-term response and the storage stability of these sensors.

13.09.6 Future Trends

13.09.6.1 Evolutionary and Revolutionary Materials

The grand challenge for enzyme-based sensors is to control the enzyme orientation in the responsive material such that the enzyme response characteristics are not affected (*325*). One of the most effective biosensor configurations reported thus far is

an enzymatic glucose sensor developed by Heller et al. in collaboration with Abbott Diabetes Care. In this configuration, an osmium hydrogel entraps the glucose dehydrogenase at one electrode (*14*,*16*). The sensor is functional over the range 20–500 mg dl^{-1}, with a correlation coefficient of $R^2 = 0.99$ against the Yellow Spring (YSI) glucose analyzer (*326*). This is regarded as an example of a third-generation biosensor, i.e., in which the enzyme is directly wired to a conductive diffusionless network. Research is now focused on materials that can improve the enzyme stability and the sensor sensitivity for other analytes, lactate, for example. It is also important to note that, with some exceptions, sensors described in the literature fail when challenged with complex samples such as interstitial fluid, sweat, and saliva. To date, the goal of a reagentless, real-time implantable sensor remains largely unachieved (*327*,*328*). As nature can carry out these complex reactions successfully, one can be inspired to continue to research, as natural ligand–biomolecule interactions are highly specific and signal transduction is fast and reversible (*327*).

Another challenge is presented by solid waste generation, able to dictate a shift from traditional polymers to 'green nanocomposites,' based on biopolymer matrices such as cellulose nanowhiskers or metal–chitosan nanocomposites (*241*,*329*). In this regard, it is worthwhile to note the ability of ILs to solubilize biopolymers such as chitosain, agarose, keratin, dextran, pectin, and cellulose is of considerable interest (*93*,*330*). For instance, Ion-Jelly® may represent a valid route for the preparation of electrochemical sensors in which the matrix stabilizes the enzyme while also providing good mechanical and electrical properties (*93*). In addition, research into biopolymers may be beneficial for providing new materials for ISE membranes (compared to the traditional PVC and polyacrylates).

Research in polymer chemistry may also provide novel materials that can allow control over the chemical, physical, and mechanical properties of sensors, and also incorporate biofunctionality (*331*). The combination of ILs with block polymers is particularly appealing as it should allow better control at the nanoscale, which may improve control over phase transitions, and mechanical and chemical properties (*332*). In addition, research into supramolecular polymers networks may help in obtaining intelligent sensors by means of noncovalent interactions via a bottom-up approach (*333*,*334*). For example, rubbery-metallo supramolecular polymers have shown self-healing by exposure to UV light, which may be an interesting feature for biosensing materials capable of self-regeneration or repair (*333*). Research is ongoing into skin-like gel behavior, wherein the signal is amplified throughout the system in response to an environmental stress or chemical input. While these studies are at an early stage, far from real applications, they may pave the way to the creation of 'artificial skin' (*335*).

Surface chemistry and nanostructuring will also be two important players in addressing the biofouling issue in biomedical applications (*264*,*336*,*337*). In order to produce long-term biocompatible coatings, the ability to trap air at the solid–liquid interface may be important (*337*). Nanostructured electrode materials will also represent a significant area of interest for kinetically controlled, surface bound reactions, e.g., glucose oxidation, which in turn will be beneficial for the development of nonenzymatic sensors (*16*).

13.09.6.2 Future Trends in Biomedical Sensing

An important challenge for materials chemistry will be the integration of sensors into wearable systems. Wearable sensors should allow the continuous monitoring of a person's physiology in a natural setting, thus decreasing the demand on local health care systems. At present, health monitoring using electronic textiles are targeting applications based on physiological parameters such as body movements or electrocardiography. Several products are already commercially available, such as the Lifeshirt®, developed by Vivometrics®, the body monitoring system developed by BodyMedia®, and the Nike-Apple iPod Sports kit, which facilitates individualized feedback control of performance during exercise periods. The use of wearable systems such as these for personalized exercise regimes for health and rehabilitation is particularly interesting. However, due to their relative complexity, there is very little activity in the development of real-time wearable chemo- and biosensing for sports applications.

These sensors require that the desired sample of analysis, usually a body fluid such as sweat or interstitial fluid, is delivered to the sensor's active surface, whereupon a reaction happens and a signal is generated. Moreover, the system must be low cost, while still being robust, miniature, flexible, washable, reusable, or disposable (*5*). All these requirements point to microfluidic devices as the key for improving wearable chemo- and biosensing (*338*). Chemical measurements on bodily fluids such as blood, sweat, and urine are needed. This area of research is still poorly developed due to the difficulty in sampling such fluids and in particular obtaining uncontaminated samples. The BIOTEX project tackled some of these problems, such as fluid handling, by developing a textile-based system to collect and analyze sweat using a textile-based sensor capable of performing chemical measurements (*5*).

Textile fibers such as cellulose or cotton can be made conductive by coating with carbon nanotubes (*339*), and antimicrobial coatings can be grafted onto textiles and plastics (*340*). Flexible, stretchable, and transparent electronics that can be intimately associated with human skin and tissues is likely to play a significant role in future applications involving chemical sensing (*236*,*341*–*345*). Currently, wearable sensors are mainly applied to the measurement of electrical activity produced by the brain and heart of humans noninvasively (*342*). Recently, Windmiller et al. (*344*) showed that on-skin tattoo electrodes can be fabricated and employed for electroanalytical measurements, though no real-time body-sensing measurements were reported. The combination of tattoo-based electrochemical sensors with wearable electronics may, in the future, assist with the realization of fully functional electronic skin (*344*,*345*). This is a most interesting and also challenging research subject, as, in principle, it may allow important parameters related to personal health to be continuously monitored in a noninvasive or minimally invasive manner (*56*).

References

1. Byrne, R.; Diamond, D. *Nat. Mater.* **2006,** *5,* 421–424.
2. Diamond, D.; Collins, F.; Cleary, J.; Zuliani, C.; Fay, C. Distributed Environmental Monitoring. In Filippini, D., Ed.; Springer, 2013; Vol. 13, p 321.
3. Byrne, R.; Ventura, C.; Benito Lopez, F.; Walther, A.; Heise, A.; Diamond, D. *Biosens. Bioelectron.* **2010,** *26,* 1392–1398.
4. De Marco, R.; Clarke, G.; Pejcic, B. *Electroanalysis* **2007,** *19,* 1987–2001.
5. Diamond, D.; Coyle, S.; Scarmagnani, S.; Hayes, J. *Chem. Rev.* **2008,** *108,* 652–679.
6. Diamond, D.; Lau, K. T.; Brady, S.; Cleary, J. *Talanta* **2008,** *75,* 606–612.
7. Farré, M.; Kantiani, L.; Pérez, S.; Barceló, D. *Trends Anal. Chem.* **2009,** *28,* 170–185.
8. Yantasee, W.; Lin, Y.; Hongsirikarn, K.; Fryxell, G. E.; Addleman, R.; Timchalk, C. *Environ. Health Perspect.* **2007,** *115,* 1683–1690.
9. Zhuiykov, S. *Sens. Actuators, B* **2012,** *161,* 1–20.
10. Ballesta Claver, J.; Valencia Miron, M. C.; Capitan-Vallvey, L. F. *Analyst* **2009,** *134,* 1423–1432.
11. Sears, M. E.; Kerr, K. J.; Bray, R. I. *J. Environ. Public Health* **2012,** 1–10.
12. Kotanen, C. N.; Moussy, F. G.; Carrara, S.; Guiseppi-Elie, A. *Biosens. Bioelectron.* **2012,** *35,* 14–26.
13. Guiseppi-Elie, A. *Anal. Bioanal. Chem.* **2011,** *399,* 403–419.
14. Heller, A.; Feldman, B. *Chem. Rev.* **2008,** *108,* 2482–2505.
15. Justin, G.; Finley, S.; Abdur Rahman, A.; Guiseppi-Elie, A. *Biomed. Microdevices* **2009,** *11,* 103–115.
16. Toghill, K. E.; Compton, R. G. *Int. J. Electrochem. Sci.* **2010,** *5,* 1246–1301.
17. Steiner, M.-S.; Duerkop, A.; Wolfbeis, O. S. *ChemInform* **2011,** *42.*
18. Hassan, S. S. M.; Badr, I. H. A.; Kamel, A. H.; Mohamed, M. S. *Anal. Sci.* **2009,** *25,* 911–917.
19. Schazmann, B.; Morris, D.; Slater, C.; Beirne, S.; Fay, C.; Reuveny, R.; Moyna, N.; Diamond, D. *Anal. Meth.* **2010,** *2,* 342–348.
20. Katsu, T.; Tsunamoto, Y.; Hanioka, N.; Komagoe, K.; Masuda, K.; Narimatsu, S. *Anal. Bioanal. Chem.* **2007,** *387,* 2057–2064.
21. Singh, P.; Singh, A. *Anal. Bioanal. Chem.* **2011,** *400,* 2261–2269.
22. Opydo-Szymaczek, J.; Opydo, J. *Biol. Trace Elem. Res.* **2010,** *137,* 159–167.
23. Al-Naimi, O.; Itota, T.; Hobson, R.; McCabe, J. *J. Mater. Sci.: Mater. Med.* **2008,** *19,* 1243–1248.
24. Singh, A. K.; Singh, U. P.; Mehtab, S.; Aggarwal, V. *Sens. Actuators, B* **2007,** *125,* 453–461.
25. Meyer, E.; Laitano, O.; Bar-Or, O.; McDougall, D.; Heigenhauser, G. J. F. *Braz. J. Med. Biol. Res.* **2007,** *40,* 135–143.
26. Venugopal, M.; Feuvrel, K. E.; Mongin, D.; Bambot, S.; Faupel, M.; Panangadan, A.; Talukder, A.; Pidva, R. *Sens. J., IEEE* **2008,** *8,* 71–80.
27. Trzebinski, J.; Sharma, S.; Radomska-Botelho Moniz, A.; Michelakis, K.; Zhang, Y.; Cass, A. E. G. *Lab Chip* **2012,** *12,* 348–352.
28. Cengiz, E.; Tamborlane, W. V. *Diabetes Technol. Ther.* **2009,** *11,* S11–S16.
29. Rebrin, K.; Sheppard, N. F.; Steil, G. M. *J. Diabetes Sci. Technol.* **2010,** *4,* 1087–1098.
30. Windmiller, J. R.; Zhou, N.; Chuang, M.-C.; Valdes-Ramirez, G.; Santhosh, P.; Miller, P. R.; Narayan, R.; Wang, J. *Analyst* **2011,** *136,* 1846–1851.
31. Yang, Y.-L.; Chuang, M.-C.; Lou, S.-L.; Wang, J. *Analyst* **2010,** *135,* 1230–1234.
32. Seoane, F.; Marquez, J. C.; Ferreira, J.; Buendia, R.; Lindecrantz, K. The Challenge of the Skin-electrode Contact in Textile-enabled Electrical Bioimpedance Measurements for Personalized Healthcare Monitoring Applications. In *Biomedical Engineering, Trends in Materials Science;* Laskovski, A. N., Ed.; In-Tech: Croatia, 2011; pp 541–546.
33. Marchand, G.; Rat, V.; Guillemaud, R.; Vinet, F.; Antonakios, M.; David, N.; Bourgerette, A. Proc. BSN 2009. Sixth International Workshop on Wearable and Implantable Body Sensor Networks, Berkeley, USA, 3–5 June 2009.
34. Paradiso, R.; Loriga, G.; Taccini, N. *IEEE Trans. Inform. Technol. Biomed.* **2005,** *9,* 337–344.
35. Aguilera-Herrador, E.; Cruz-Vera, M.; Valcarcel, M. *Analyst* **2010,** *135,* 2220–2232.
36. Gonzalo-Ruiz, J.; Mas, R.; de Haro, C.; Cabruja, E.; Camero, R.; Alonso-Lomillo, M. A.; Muñoz, F. J. *Biosens. Bioelectron.* **2009,** *24,* 1788–1791.
37. Li, C.; Shutter, L. A.; Wu, P.-M.; Ahn, C. H.; Narayan, R. K. *Lab Chip* **2010,** *10,* 1476–1479.
38. Heinrich, S.; Luppa, M.; Matschinger, H.; Angermeyer, M. C.; Riedel-Heller, S. G.; Koenig, H.-H. *Value in Health* **2008,** *11,* 611–620.
39. Rahman, M. M.; Shiddiky, M. J. A.; Rahman, M. A.; Shim, Y.-B. *Anal. Biochem.* **2009,** *384,* 159–165.
40. Ges, I. A.; Baudenbacher, F. *Biosens. Bioelectron.* **2010,** *26,* 828–833.
41. Lupu, S.; Lakard, B.; Hihn, J.-Y.; Dejeu, J.; Rougeot, P.; Lallemand, S. *Thin Solid Films* **2011,** *519,* 7754–7762.
42. Romero, M. R.; Ahumada, F.; Garay, F.; Baruzzi, A. M. *Anal. Chem.* **2010,** *82,* 5568–5572.
43. Schabmueller, C. G. J.; Loppow, D.; Piechotta, G.; Schütze, B.; Albers, J.; Hintsche, R. *Biosens. Bioelectron.* **2006,** *21,* 1770–1776.
44. Romero, M. R.; Garay, F.; Baruzzi, A. M. *Sens. Actuators, B* **2008,** *131,* 590–595.
45. Yashina, E. I.; Borisova, A. V.; Karyakina, E. E.; Shchegolikhina, O. I.; Vagin, M. Y.; Sakharov, D. A.; Tonevitsky, A. G.; Karyakin, A. A. *Anal. Chem.* **2010,** *82,* 1601–1604.
46. Gomathi, P.; Ragupathy, D.; Choi, J. H.; Yeum, J. H.; Lee, S. C.; Kim, J. C.; Lee, S. H.; Ghim, H. D. *Sens. Actuators, B* **2011,** *153,* 44–49.
47. Lakard, B.; Magnin, D.; Deschaume, O.; Vanlancker, G.; Glinel, K.; Demoustier-Champagne, S.; Nysten, B.; Jonas, A. M.; Bertrand, P.; Yunus, S. *Biosens. Bioelectron.* **2011,** *26,* 4139–4145.
48. Wolfe, R. A.; Ashby, V. B.; Daugirdas, J. T.; Agodoa, L. Y. C.; Jones, C. A.; Port, F. K. *Am. J. Kidney Dis.* **2000,** *36,* 1025.
49. Hibbard, T.; Killard, A. J. *Crit. Rev. Anal. Chem.* **2011,** *41,* 21–35.
50. Kumar, C.; Patel, N. *Gases Technol.* **2002,** *1,* 24–30.
51. Rahman, M. A.; Lee, K.-S.; Park, D.-S.; Won, M.-S.; Shim, Y.-B. *Biosens. Bioelectron.* **2008,** *23,* 857–864.
52. Wang, C.; Wang, G.; Fang, B. *Microchim. Acta* **2009,** *164,* 113–118.
53. Peng, Y.; Ji, Y.; Zheng, D.; Hu, S. *Sens. Actuators, B* **2009,** *137,* 656–661.
54. Phair, J.; Newton, L.; McCormac, C.; Cardosi, M. F.; Leslie, R.; Davis, J. *Analyst* **2011,** *136,* 4692–4695.
55. Lynch, A.; Diamond, D.; Leader, M. *Analyst* **2000,** *125,* 2264–2267.
56. Coyle, S.; Lau, K. T.; Moyna, N.; O'Gorman, D.; Diamond, D.; Di Francesco, F.; Costanzo, D.; Salvo, P.; Trivella, M. G.; De Rossi, D. E.; Taccini, N.; Paradiso, R.; Porchet, J. A.; Ridolfi, A.; Luprano, J.; Chuzel, C.; Lanier, T.; Revol-Cavalier, F.; Schoumacker, S.; Mourier, V.; Chartier, I.; Convert, R.; De-Moncuit, H.; Bini, C. *IEEE T. Inf. Technol. Biomed.* **2010,** *14,* 364–370.
57. Munaron, L.; Scianna, M. *World J. Biol. Chem.* **2012,** *3,* 1211–1226.
58. Titze, J.; Machnik, A. *Curr. Opin. Nephrol. Hypertens.* **2010,** *19,* 385–392.
59. Brugnara, C. *Clin. Chem.* **2003,** *10,* 1573–1578.
60. Spielmann, N.; Wong, D. T. *Oral Dis.* **2011,** *17,* 345–354.
61. Malongo, T. K.; Patris, S.; Macours, P.; Cotton, F.; Nsangu, J.; Kauffmann, J.-M. *Talanta* **2008,** *76,* 540–547.
62. Kim, S.; Park, J. W.; Kim, D.; Kim, D.; Lee, I.-H.; Jon, S. *Angew. Chem., Int. Ed.* **2009,** *48,* 4138–4141.
63. Makarychev-Mikhailov, S.; Shvarev, A.; Bakker, E. New Trends in Ion-selective Electrodes. In *Electrochemical Sensors, Biosensors and Their Biomedical Applications;* Zhang, X., Ju, H., Wang, J., Eds.; Academic Press: US, 2007; pp 72–114.
64. Lewenstam, A. Clinical Analysis of Blood Gases and Electrolytes by Ion-selective Sensors. In *Electrochemical Sensor Analysis*; Alegret, S., Merkoçi, A., Eds.; Elsevier: Amsterdam, The Netherlands, 2007; Vol. 49, pp 5–24.

65. Harvey, C. J.; LeBouf, R. F.; Stefaniak, A. B. *Toxicol. in Vitro* **2010,** *24,* 1790–1796.
66. Souza, A. P. R.d.; Lima, A. S.; Salles, M. O.; Nascimento, A. N.; Bertotti, M. *Talanta* **2010,** *83,* 167–170.
67. Zietz, B. P.; Dieter, H. H.; Lakomek, M.; Schneider, H.; Keßler-Gaedtke, B.; Dunkelberg, H. *Sci. Total Environ.* **2003,** *302,* 127–144.
68. Rivera-Mancía, S.; Pérez-Neri, I.; Ríos, C.; Tristán-López, L.; Rivera-Espinosa, L.; Montes, S. *Chem.-Biol. Interact.* **2010,** *186,* 184–199.
69. Schuhmann, W.; Bonsen, E. M. Biosensors. In *Encyclopedia of Electrochemistry: Instrumentation and Electroanalytical Chemistry;* Bard, A. J., Stratmann, M., Unwin, P. R., Eds.; Wiley-VCH: Weinheim, Germany, 2003; pp 350–383.
70. Bard, A. J.; Faulkner, L. R. Electrochemical Instrumentation. In *Electrochemical Methods: Fundamentals and Applications;* Wiley India Pvt. Ltd.: New York, 2006; pp 632–658.
71. Wipf, D. Analog and Digital Instrumentation. In *Handbook of Electrochemistry;* Zoski, C. G., Ed.; Elsevier: Amsterdam, The Netherlands, 2007; pp 24–50.
72. Liu, H.; Crooks, R. M. *Anal. Chem.* **2012,** *84,* 2528–2532.
73. Guiseppi-Elie, A. *Biomaterials* **2010,** *31,* 2701–2716.
74. Yang, X.; Pan, X.; Blyth, J.; Lowe, C. R. *Biosens. Bioelectron.* **2008,** *23,* 899–905.
75. Martinez-Manez, R.; Sancenon, F.; Biyikal, M.; Hecht, M.; Rurack, K. *J. Mater. Chem.* **2011,** *21,* 12588–12604.
76. Fries, K. H.; Driskell, J. D.; Sheppard, G. R.; Locklin, J. *Langmuir* **2011,** *27,* 12253–12260.
77. Balogh, D.; Tel-Vered, R.; Freeman, R.; Willner, I. *J. Am. Chem. Soc.* **2011,** *133,* 6533–6536.
78. Yehezkeli, O.; Tel-Vered, R.; Reichlin, S.; Willner, I. *ACS Nano* **2011,** *5,* 2385–2391.
79. Gamero, M.; Pariente, F.; Lorenzo, E.; Alonso, C. *Biosens. Bioelectron.* **2010,** *25,* 2038–2044.
80. Fraser, K. J.; MacFarlane, D. R. *Aust. J. Chem.* **2009,** *62,* 309–321.
81. Hough, W. L.; Smiglak, M.; Rodriguez, H.; Swatloski, R. P.; Spear, S. K.; Daly, D. T.; Pernak, J.; Grisel, J. E.; Carliss, R. D.; Soutullo, M. D.; Davis, J. J. H.; Rogers, R. D. *New J. Chem.* **2007,** *31,* 1429–1436.
82. Forsyth, S. A.; Pringle, J. M.; MacFarlane, D. R. *Aust. J. Chem.* **2004,** *57,* 113–119.
83. Hapiot, P.; Lagrost, C. *Chem. Rev.* **2008,** *108,* 2238–2264.
84. Buzzeo, M. C.; Evans, R. G.; Compton, R. G. *ChemPhysChem* **2004,** *5,* 1106–1120.
85. MacFarlane, D. R.; Pringle, J. M.; Johansson, K. M.; Forsyth, S. A.; Forsyth, M. *Chem. Commun.* **2006,** 1905–1917.
86. Wei, D.; Ivaska, A. *Anal. Chim. Acta* **2008,** *607,* 126–135.
87. Erdmenger, T.; Guerrero-Sanchez, C.; Vitz, J.; Hoogenboom, R.; Schubert, U.S. *Chem. Soc. Rev.* **2010,** *39,* 3317.
88. Armand, M.; Endres, F.; MacFarlane, D. R.; Ohno, H.; Scrosati, B. *Nat. Mater.* **2009,** *8,* 621–629.
89. Franzoi, A. C.; Migowski, P.; Dupont, J.; Vieira, I. C. *Anal. Chim. Acta* **2009,** *639,* 90–95.
90. Keskin, S.; Kayrak-Talay, D.; Akman, U.; Hortacsu, O. *J. Supercrit. Fluids* **2007,** *43,* 150–180.
91. Torimoto, T.; Tsuda, T.; Okazaki, K.-i.; Kuwabata, S. *Adv. Mater.* **2010,** *22,* 1196–1221.
92. Ohno, H. *Electrochemical Aspects of Ionic Liquids;* John Wiley & Sons, Inc: Hoboken, NJ, 2005.
93. Singh, T.; Trivedi, T. J.; Kumar, A. *Green Chem.* **2010,** *12,* 1029–1035.
94. Davis, J. J. H.; Fox, P. A. *Chem. Commun.* **2003,** 1209–1212.
95. Le Bideau, J.; Viau, L.; Vioux, A. *Chem. Soc. Rev.* **2011,** *40,* 907–925.
96. Ducros, J. B.; Buchtova, N.; Magrez, A.; Chauvet, O.; Le Bideau, J. *J. Mater. Chem.* **2011,** *21,* 2508–2511.
97. MacFarlane, D. R.; Forsyth, M.; Howlett, P. C.; Pringle, J. M.; Sun, J.; Annat, G.; Neil, W.; Izgorodina, E. I. *Acc. Chem. Res.* **2007,** *40,* 1165–1173.
98 Suarez, P. A. Z.; Selbach, V. M.; Dullius, J. E. L.; Einloft, S.; Piatnicki, C. M. S.; Azambuja, D. S.; de Souza, R. F.; Dupont, J. *Electrochim. Acta* **1997,** *42,* 2533–2535.
99. Taylor, A. W.; Licence, P.; Abbott, A. P. *Phys. Chem. Chem. Phys.* **2011,** *13,* 10147–10154.
100. Kavanagh, A.; Fraser, K. J.; Byrne, R.; Diamond, D. *ACS Appl. Mater. Interfaces* **2012,** *5,* 55–62.
101. Zeng, X.; Li, X.; Xing, L.; Liu, X.; Luo, S.; Wei, W.; Kong, B.; Li, Y. *Biosens. Bioelectron.* **2009,** *24,* 2898–2903.
102. Fujita, K.; MacFarlane, D. R.; Forsyth, M.; Yoshizawa-Fujita, M.; Murata, K.; Nakamura, N.; Ohno, H. *Biomacromolecules* **2007,** *8,* 2080–2086.
103. Byrne, N.; Wang, L.-M.; Belieres, J.-P.; Angell, C. A. *Chem. Commun.* **2007,** 2714–2716.
104. Yang, S. Y.; Cicoira, F.; Byrne, R.; Benito-Lopez, F.; Diamond, D.; Owens, R. M.; Malliaras, G. G. *Chem. Commun.* **2010,** *46,* 7972–7974.
105. Berggren, M.; Nilsson, D.; Robinson, N. D. *Nat. Mater.* **2007,** *6,* 3–5.
106. Zhao, H. *J. Chem. Technol. Biotechnol.* **2010,** *85,* 891–907.
107. Moniruzzaman, M.; Kamiya, N.; Goto, M. *Org. Biomol. Chem.* **2010,** *8,* 2887–2899.
108. Weingartner, H.; Cabrele, C.; Herrmann, C. *Phys. Chem. Chem. Phys.* **2012,** *14,* 415–426.
109. Yang, Z. *J. Biotechnol.* **2009,** *144,* 12–22.
110. Musameh, M. M.; Kachoosangi, R. T.; Xiao, L.; Russell, A.; Compton, R. G. *Biosens. Bioelectron.* **2008,** *24,* 87–92.
111. Ping, J.; Wu, J.; Ying, Y. *Electrochem. Commun.* **2010,** *12,* 1738–1741.
112. Ping, J.; Wang, Y.; Fan, K.; Wu, J.; Ying, Y. *Biosens. Bioelectron.* **2011,** *28,* 204–209.
113. Santafé, A.I. A. M.; Doumèche, B.; Blum, L. J.; Girard-Egrot, A.s. P.; Marquette, C. A. *Anal. Chem.* **2010,** *82,* 2401–2404.
114. Zuliani, C.; Diamond, D. *Electrochim. Acta* **2012,** *84,* 29–34.
115. Cicmil, D.; Anastasova, S.; Kavanagh, A.; Diamond, D.; Mattinen, U.; Bobacka, J.; Lewenstam, A.; Radu, A. *Electroanalysis* **2011,** *23,* 1881–1890.
116. Zhang, T.; Lai, C.-Z.; Fierke, M. A.; Stein, A.; Bühlmann, P. *Anal. Chem.* **2012,** *84,* 7771–7778.
117. Guth, U.; Gerlach, F.; Decker, M.; Oelßner, W.; Vonau, W. *J. Solid State Electrochem.* **2009,** *13,* 27–39.
118. Kakiuchi, T.; Yoshimatsu, T.; Nishi, N. *Anal. Chem.* **2007,** *79,* 7187–7191.
119. Gourishetty, R.; Crabtree, A. M.; Sanderson, W. M.; Johnson, R. D. *Anal. Bioanal. Chem.* **2011,** *400,* 3025–3033.
120. Shvedene, N. V.; Chernyshov, D. V.; Khrenova, M. G.; Formanovsky, A. A.; Baulin, V. E.; Pletnev, I. V. *Electroanalysis* **2006,** *18,* 1416–1421.
121. Marciniak, A. *Int. J. Mol. Sci.* **2010,** *11,* 1973–1990.
122. Coll, C.; Labrador, R. H.; Manez, R. M.; Soto, J.; Sancenon, F.; Segui, M. J. *Chem. Commun.* **2005,** *24,* 3033–3035.
123. Chernyshov, D. V.; Egorov, V. M.; Shvedene, N. V.; Pletnev, I. V. *ACS Appl. Mater. Interfaces* **2009,** *1,* 2055–2059.
124. Wardak, C. *J. Hazard. Mater.* **2011,** *186,* 1131–1135.
125. Wardak, C. *Electroanalysis* **2012,** *24,* 85–90.
126. Wang, K. F.; Zhang, L.; Zhuang, R. R.; Jian, F. F. *Transition Met. Chem.* **2011,** *36,* 785–791.
127. Delker, D.; Hatch, G.; Allen, J.; Crissman, B.; George, M.; Geter, D.; Kilburn, S.; Moore, T.; Nelson, G.; Roop, B.; Slade, R.; Swank, A.; Ward, W.; DeAngelo, A. *Toxicology* **2006,** *221,* 158–165.
128. Bryan, N. S.; Alexander, D. D.; Coughlin, J. R.; Milkowski, A. L.; Boffetta, P. *Food Chem. Toxicol.* **2012,** *50,* 3646–3665.
129. Plieth, W. Intrinsically Conducting Polymers. In *Electrochemistry for Materials Science;* Elsevier: Hungary, 2008; pp 323–363.
130. Bidan, G. Electropolymerized Films of Pi-conjugated Polymers. A Tool for Surface Functionalization: A Brief Historical Evolution and Recent Trends. In *Electropolymerization: Concepts, Materials and Applications;* Cosnier, S., Karyakin, A., Eds.; John Wiley & Sons: Germany, 2010; pp 1–26.
131. Otero, T. F.; Arias-Pardilla, J. Electrochemical Devices: Artificial Muscles. In *Electropolymerization: Concepts, Materials and Applications;* Cosnier, S., Karyakin, A., Eds.; John Wiley & Sons: Germany, 2010; pp 241–245.

132. Vorotyntsev, M. A.; Zinovyeva, V. A.; Konev, D. V. Mechanism of Electropolymerization and Redox Activity: Fundamental Aspects. In *Electropolymerization: Concepts, Materials and Applications;* Cosnier, S., Karyakin, A., Eds.; John Wiley & Sons: Germany, 2010; pp 27–50.
133. Campbell, J. S. History of Conductive Polymers. In *Nanostructured Conductive Polymers;* Eftekhari, A., Ed.; Wiley: Great Britain, 2011; pp 1–17.
134. Chujo, Y. *Conjugated Polymer Synthesis;* Wiley: Hoboken, NJ, 2011.
135. Leclerc, M.; Morin, J. F. *Design and Synthesis of Conjugated Polymers;* Wiley: Weinheim, 2010.
136. Cosnier, S.; Karyakin, A. *Electropolymerization;* Wiley, 2011.
137. Wallace, G. G.; Spinks, G. M.; Kane-Maguire, L. A. P. *Conductive Electroactive Polymers: Intelligent Polymer Systems;* CRC Press: Boca Raton, FL, 2009.
138. Eftekhari, A. *Nanostructured Conductive Polymers;* Wiley: Hoboken, NJ, 2011.
139. Skotheim, T. A.; Reynolds, J. R. *Handbook of Conducting Polymers;* CRC: Boca Raton, FL, 2007.
140. Gerard, M.; Chaubey, A.; Malhotra, B. D. *Biosens. Bioelectron.* **2002,** *17,* 345–359.
141. Lin, P.; Yan, F. *Adv. Mater.* **2012,** *24,* 34–51.
142. Nambiar, S.; Yeow, J. T. W. *Biosens. Bioelectron.* **2011,** *26,* 1825–1832.
143. Ates, M.; Sarac, A. S. *Prog. Org. Coat.* **2009,** *66,* 337–358.
144. Rozlosnik, N. *Anal. Bioanal. Chem.* **2009,** *395,* 637–645.
145. Snook, G. A.; Best, A. S. *J. Mater. Chem.* **2009,** *19,* 4248–4254.
146. Ahmad, S.; Deepa, M.; Singh, S. *Langmuir* **2007,** *23,* 11430–11433.
147. Marjanovic, G. C. Polyaniline Nanostructures. In *Nanostructured Conductive Polymers;* Eftekhari, A., Ed.; Wiley: Chichester, UK, 2011; pp 19–98.
148. Suman; O'Reilly, E.; Kelly, M.; Morrin, A.; Smyth, M. R.; Killard, A. J. *Anal. Chim. Acta* **2011,** *697,* 98–102.
149. Sriprachuabwong, C.; Karuwan, C.; Wisitsorrat, A.; Phokharatkul, D.; Lomas, T.; Sritongkham, P.; Tuantranont, A. *J. Mater. Chem.* **2012,** *22,* 5478–5485.
150. Ahmad, S.; Carstens, T.; Berger, R.; Butt, H.-J.; Endres, F. *Nanoscale* **2011,** *3,* 251–257.
151. Long, Y.-Z.; Li, M.-M.; Gu, C.; Wan, M.; Duvail, J.-L.; Liu, Z.; Fan, Z. *Prog. Polym. Sci.* **2011,** *36,* 1415–1442.
152. Wan, M. *Adv. Mater.* **2008,** *20,* 2926–2932.
153. Lu, W.; Fadeev, A. G.; Qi, B.; Smela, E.; Mattes, B. R.; Ding, J.; Spinks, G. M.; Mazurkiewicz, J.; Zhou, D.; Gordon, G. W.; MacFarlane, D. R.; Forsyth, S. A.; Forsyth, M. *Science* **2002,** *297,* 983–987.
154. Winterton, N. *J. Mater. Chem.* **2006,** *16,* 4281–4293.
155. Jiang, Y.; Wang, A.; Kan, J. *Sens. Actuators, B* **2007,** *124,* 529–534.
156. Ahmad, S.; Yum, J.-H.; Xianxi, Z.; Gratzel, M.; Butt, H.-J.; Nazeeruddin, M. K. *J. Mater. Chem.* **2010,** *20,* 1654–1658.
157. Li, Y.; Wang, B.; Chen, H.; Feng, W. *J. Power Sources* **2010,** *195,* 3025–3030.
158. Nien, P.-C.; Tung, T.-S.; Ho, K.-C. *Electroanalysis* **2006,** *18,* 1408–1415.
159. Emre, F. B.; Ekiz, F.; Balan, A.; Emre, S.; Timur, S.; Toppare, L. *Sens. Actuators, B* **2011,** *158,* 117–123.
160. Alvin Koh, W. C.; Rahman, M. A.; Choe, E. S.; Lee, D. K.; Shim, Y.-B. *Biosens. Bioelectron.* **2008,** *23,* 1374–1381.
161. Kausaite-Minkstimiene, A.; Mazeiko, V.; Ramanaviciene, A.; Ramanavicius, A. *Biosens. Bioelectron.* **2010,** *26,* 790–797.
162. Aguilar, A. D.; Forzani, E. S.; Nagahara, L. A.; Amlani, I.; Tsui, R.; Tao, N. J. *Sens. J., IEEE* **2008,** *8,* 269–273.
163. Lu, L.-M.; Wang, S.-P.; Qu, F.-L.; Zhang, X.-B.; Huan, S.; Shen, G.-L.; Yu, R.-Q. *Electroanalysis* **2009,** *21,* 1152–1158.
164. Wang, J.; Mo, X.; Ge, D.; Tian, Y.; Wang, Z.; Wang, S. *Synth. Met.* **2006,** *156,* 514–518.
165. Zang, J.; Li, C. M.; Bao, S.-J.; Cui, X.; Bao, Q.; Sun, C. Q. *Macromolecules* **2008,** *41,* 7053–7057.
166. Özcan, L.; Şahin, Y.; Türk, H. *Biosens. Bioelectron.* **2008,** *24,* 512–517.
167. Zang, J.; Bao, S.-J.; Li, C. M.; Bian, H.; Cui, X.; Bao, Q.; Sun, C. Q.; Guo, J.; Lian, K. *J. Phys. Chem. C* **2008,** *112,* 14843–14847.
168. Debiemme-Chouvy, C. *Electrochem. Commun.* **2009,** *11,* 298–301.
169. Zhang, X.; Wang, J.; Wang, Z.; Wang, S.c. *J. Macromol. Sci., Part B* **2006,** *45,* 475–483.
170. Zhang, Y.; Sun, X. *Chem. Commun.* **2011,** *47,* 3927–3929.
171. Luo, X.; Lee, I.; Huang, J.; Yun, M.; Cui, X. T. *Chem. Commun.* **2011,** *47,* 6368–6370.
172. Bluth, M. *Cancer Immunol. Immunother.* **2012,** *61,* 1585–1590.
173. Wanekaya, A. K.; Chen, W.; Myung, N. V.; Mulchandani, A. *Electroanalysis* **2006,** *18,* 533–550.
174. Bobacka, J.; Ivaska, A. Ion Sensors with Conducting Polymers as Ion-to-electron Transducers. In *Electrochemical Sensor Analysis, Part 1 Fundamentals and Applications*; Alegret, S., Merkoçi, A., Eds.; Elsevier: Amsterdam, The Netherlands, 2007; Vol. 49, pp 73–86.
175. Bobacka, J. *Electroanalysis* **2006,** *18,* 7–18.
176. Bobacka, J.; Ivaska, A.; Lewenstam, A. *Chem. Rev.* **2008,** *108,* 329–351.
177. Lindner, E.; Gyurcsányi, R. *J. Solid State Electrochem.* **2009,** *13,* 51–68.
178. Pawlak, M.; Grygolowicz-Pawlak, E.; Bakker, E. *Anal. Chem.* **2010,** *82,* 6887–6894.
179. Amemiya, S. Potentiometric Ion-selective Electrodes. In *Handbook of Electrochemistry;* Zoski, C. G., Ed.; Elsevier: Amsterdam, The Netherlands, 2007; pp 261–294.
180. Vázquez, M.; Danielsson, P.; Bobacka, J.; Lewenstam, A.; Ivaska, A. *Sens. Actuators, B* **2004,** *97,* 182–189.
181. Lindfors, T.; Höfler, L.; Jágerszki, G.; Gyurcsányi, R. E. *Anal. Chem.* **2011,** *83,* 4902–4908.
182. Lindfors, T.; J.I. Szücs; Sundfors, F.; Gyurcsányi, R. E. *Anal. Chem.* **2010,** *82,* 9425–9432.
183. Radu, A.; Diamond, D. Ion-selective Electrodes in Trace Level Analysis of Heavy Metals: Potentiometry for the XXI Century. In *Comprehensive Analytical Chemistry*; Alegret, S., Merkoçi, A., Eds.; Elsevier: Amsterdam, The Netherlands, 2007; Vol. 49, pp 25–52.
184. Guo, J.; Amemiya, S. *Anal. Chem.* **2006,** *78,* 6893–6902.
185. Michalska, A.; Wojciechowski, M.; Bulska, E.; Maksymiuk, K. *Talanta* **2010,** *82,* 151–157.
186. Michalska, A.; Wojciechowski, M.; Jedral, W.; Bulska, E.; Maksymiuk, K. *J. Solid State Electrochem.* **2009,** *13,* 99–106.
187. Chumbimuni-Torres, K. Y.; Rubinova, N.; Radu, A.; Kubota, L. T.; Bakker, E. *Anal. Chem.* **2006,** *78,* 1318–1322.
188. Han, W. S.; Lee, Y. H.; Jung, K. J.; Ly, S. Y.; Hong, T. K.; Kim, M. H. *J. Anal. Chem.* **2008,** *63,* 987.
189. Lisak, G.; Wagner, M.; Kvarnstrom, C.; Bobacka, J.; Ivaska, A.; Lewenstam, A. *Electroanalysis* **2010,** *22,* 2794–2800.
190. Kisiel, A.; Mazur, M.; Kuśnieruk, S.; Kijewska, K.; Krysiński, P.; Michalska, A. *Electrochem. Commun.* **2010,** *12,* 1568–1571.
191. Kijewska, K.; Blanchard, G. J.; Szlachetko, J.; Stolarski, J.; Kisiel, A.; Michalska, A.; Maksymiuk, K.; Pisarek, M.; Majewski, P.; Krysinski, P.; Mazur, M. *Chem. – Eur. J.* **2012,** *18,* 310–320.
192. Malinowski, P.; Grzegrzółka, I.; Michalska, A.; Maksymiuk, K. *J. Solid State Electrochem.* **2010,** *14,* 2027–2037.
193. Garcia-Cordova, F.; Valero, L.; Ismail, Y. A.; Otero, T. F. *J. Mater. Chem.* **2011,** *21,* 17265–17272.
194. Mohadesi, A.; Taher, M. A. *Anal. Sci.* **2007,** *23,* 969.
195. Mao, H.; Liu, X.; Chao, D.; Cui, L.; Li, Y.; Zhang, W.; Wang, C. *J. Mater. Chem.* **2010,** *20,* 10277.
196. Dwivedi, A. K.; Saikia, G.; Iyer, P. K. *J. Mater. Chem.* **2011,** *21,* 2502–2507.
197. Schmid, G. *Nanoparticles: From Theory to Application;* Wiley, 2011.
198. Brust, M.; Walker, M.; Bethell, D.; Schiffrin, D. J.; Whyman, R. *J. Chem. Soc. Chem. Commun.* **1994,** *0,* 801–802.
199. Rao, C. N. R.; Kulkarni, G. U.; Thomas, P. J.; Edwards, P. P. *Chem. Soc. Rev.* **2000,** *29,* 27–35.

200. Jia, C.-J.; Schuth, F. *Phys. Chem. Chem. Phys.* **2011,** *13,* 2457–2487.
201. Haes, A. J.; Zou, S.; Schatz, G. C.; Van Duyne, R. P. *J. Phys. Chem. B* **2003,** *108,* 109–116.
202. Kelly, K. L.; Coronado, E.; Zhao, L. L.; Schatz, G. C. *J. Phys. Chem. B* **2002,** *107,* 668–677.
203. Narayanan, R.; El-Sayed, M. A. *J. Phys. Chem. B* **2005,** *109,* 12663–12676.
204. Murray, R. W. *Chem. Rev.* **2008,** *108,* 2688–2720.
205. Rotello, V. M. *Nanoparticles;* Kluwer Academic Pub: New York, 2004.
206. Nagarajan, R.; Hatton, T. A. *A.C.S.D.o. Colloid, S. Chemistry, A.C.S. Meeting, Nanoparticles: Synthesis, Stabilization, Passivation, and Functionalization;* American Chemical Society, 2008.
207. Anderson, L. J. E.; Payne, C. M.; Zhen, Y.-R.; Nordlander, P.; Hafner, J. H. *Nano Lett.* **2011,** *11,* 5034–5037.
208. Strong, L. E.; West, J. L. *Wiley Interdiscip. Rev.: Nanomed. Nanobiotechnol.* **2011,** *3,* 307–317.
209. Campbell, F.; Compton, R. *Anal. Bioanal. Chem.* **2010,** *396,* 241–259.
210. You, C.-C.; Miranda, O. R.; Gider, B.; Ghosh, P. S.; Kim, I.-B.; Erdogan, B.; Krovi, S. A.; Bunz, U. H. F.; Rotello, V. M. *Nat. Nano* **2007,** *2,* 318–323.
211. Jaworska, E.; Wójcik, M.; Kisiel, A.; Mieczkowski, J.; Michalska, A. *Talanta* **2011,** *85,* 1986–1989.
212. González, E.; Arbiol, J.; Puntes, V. F. *Science* **2011,** *334,* 1377–1380.
213. Zhou, Y.-G.; Rees, N. V.; Compton, R. G. *Chem. Phys. Lett.* **2011,** *511,* 183–186.
214. Wojcik, M.; Lewandowski, W.; Matraszek, J.; Mieczkowski, J.; Borysiuk, J.; Pociecha, D.; Gorecka, E. *Angew. Chem., Int. Ed.* **2009,** *48,* 5167–5169.
215. Zhao, Y.; Thorkelsson, K.; Mastroianni, A. J.; Schilling, T.; Luther, J. M.; Rancatore, B. J.; Matsunaga, K.; Jinnai, H.; Wu, Y.; Poulsen, D.; Frechet, J. M. J.; Paul Alivisatos, A.; Xu, T. *Nat. Mater.* **2009,** *8,* 979–985.
216. Sia, S. K.; Kricka, L. J. *Lab Chip* **2008,** *8,* 1982–1983.
217. Martinez, A. W.; Phillips, S. T.; Butte, M. J.; Whitesides, G. M. *Angew. Chem., Int. Ed.* **2007,** *46,* 1318–1320.
218. Schilling, K. M.; Lepore, A. L.; Kurian, J. A.; Martinez, A. W. *Anal. Chem.* **2012,** *84,* 1579–1585.
219. Songjaroen, T.; Dungchai, W.; Chailapakul, O.; Henry, C. S.; Laiwattanapaisal, W. *Lab Chip* **2012,** *12,* 3392–3398.
220. Li, H. X.; Rothberg, L. J. *J. Am. Chem. Soc.* **2004,** *126,* 10958–10961.
221. Sharon, E.; Freeman, R.; Tel-Vered, R.; Willner, I. *Electroanalysis* **2009,** *21,* 1291–1296.
222. Zhang, J.; Wang, L.; Pan, D.; Song, S.; Boey, F. Y. C.; Zhang, H.; Fan, C. *Small* **2008,** *4,* 1196–1200.
223. Golub, E.; Pelossof, G.; Freeman, R.; Zhang, H.; Willner, I. *Anal. Chem.* **2009,** *81,* 9291–9298.
224. Zhu, Z.; Wu, C.; Liu, H.; Zou, Y.; Zhang, X.; Kang, H.; Yang, C. J.; Tan, W. *Angew. Chem., Int. Ed.* **2010,** *49,* 1052–1056.
225. Yu, C.; Tseng, W. *Langmuir* **2008,** *24,* 12717.
226. Zhou, Y.; Wang, S.; Zhang, K.; Jiang, X. *Angew. Chem., Int. Ed.* **2008,** *47,* 7454–7456.
227. Jiang, Y.; Zhao, H.; Lin, Y.; Zhu, N.; Ma, Y.; Mao, L. *Angew. Chem., Int. Ed.* **2010,** *49,* 4800–4804.
228 Xia, F.; Zuo, X.; Yang, R.; Xiao, Y.; Kang, D.; Valle-Belisle, A.; Gong, X.; Yuen, J. D.; Hsu, B. B. Y.; Heeger, A. J.; Plaxco, K. W. *Proc. Natl. Acad. Sci.* **2010,** *107,* 10837–10841.
229. Liu, X.; Dai, Q.; Austin, L.; Coutts, J.; Knowles, G.; Zou, J.; Chen, H.; Huo, Q. *J. Am. Chem. Soc.* **2008,** *130,* 2780–2782.
230. Ambrosi, A.; Airò, F.; Merkoci, A. *Anal. Chem.* **2009,** *82,* 1151–1156.
231. Rodriguez-Lorenzo, L.; de la Rica, R.; Alvarez-Puebla, R. A.; Liz-Marzan, L. M.; Stevens, M. M. *Nat. Mater.* **2012,** *11,* 604–607.
232. Panfilova, E.; Shirokov, A.; Khlebtsov, B.; Matora, L.; Khlebtsov, N. *Nano Res.* **2012,** *5,* 124–134.
233. Strömberg, N.; Hakonen, A. *Anal. Chim. Acta* **2011,** *704,* 139–145.
234. Zhang, J.; Xu, X.; Yang, C.; Yang, F.; Yang, X. *Anal. Chem.* **2011,** *83,* 3911.
235. Feng, M.; Han, H.; Zhang, J.; Tachikawa, H. Electrochemical Sensors Based on Carbon Nanotubes. In *Electrochemical Sensors, Biosensors and Their Biomedical Applications;* Zhang, X., Ju, H., Wang, J., Eds.; Academic Press: Amsterdam, The Netherlands; Boston, MA, 2007; pp 459–500.
236. Cao, Q.; Rogers, J. A. *Adv. Mater.* **2009,** *21,* 29–53.
237. Goran, J. M.; Lyon, J. L.; Stevenson, K. J. *Anal. Chem.* **2011,** *83,* 8123–8129.
238. Jönsson-Niedziolka, M.; Kaminska, A.; Opallo, M. *Electrochim. Acta* **2010,** *55,* 8744–8750.
239. Zeng, X.; Li, X.; Liu, X.; Liu, Y.; Luo, S.; Kong, B.; Yang, S.; Wei, W. *Biosens. Bioelectron.* **2009,** *25,* 896–900.
240. Vashist, S. K.; Zheng, D.; Al-Rubeaan, K.; Luong, J. H. T.; Sheu, F.-S. *Biotechnol. Adv.* **2011,** *29,* 169–188.
241. Inamdar, N.; Mourya, V. K. Composite of Chitosan for Biomedical Applications. In *Recent Developments in Bio-nanocomposites for Biomedical Applications;* Tiwari, A., Ed.; Nova Science Publishers: New York, 2011; pp 277–343.
242. Kim, K. S.; Zhao, Y.; Jang, H.; Lee, S. Y.; Kim, J. M.; Ahn, J. H.; Kim, P.; Choi, J. Y.; Hong, B. H. *Nature* **2009,** *457,* 706–710.
243. Tlili, C.; Myung, N. V.; Shetty, V.; Mulchandani, A. *Biosens. Bioelectron.* **2011,** *26,* 4382–4386.
244. Ohno, Y.; Maehashi, K.; Matsumoto, K. *J. Am. Chem. Soc.* **2010,** *132,* 18012–18013.
245. Grieshaber, D.; MacKenzie, R.; Vörös, J.; Reimhult, E. *Sensors* **2008,** *8,* 1400–1458.
246. Janata, J.; Josowicz, M. *Nat. Mater.* **2003,** *2,* 19–24.
247. Goldsmith, B. R.; Mitala, J. J.; Josue, J.; Castro, A.; Lerner, M. B.; Bayburt, T. H.; Khamis, S. M.; Jones, R. A.; Brand, J. G.; Sligar, S. G.; Luetje, C. W.; Gelperin, A.; Rhodes, P. A.; Discher, B. M.; Johnson, A. T. C. *ACS Nano* **2011,** *5,* 5408–5416.
248. Cella, L. N.; Chen, W.; Myung, N. V.; Mulchandani, A. *J. Am. Chem. Soc.* **2010,** *132,* 5024–5026.
249. An, T.; Kim, K. S.; Hahn, S. K.; Lim, G. *Lab Chip* **2010,** *10,* 2052–2056.
250. Lee, D.; Cui, T. *Biosens. Bioelectron.* **2010,** *25,* 2259–2264.
251. Ohno, Y.; Maehashi, K.; Yamashiro, Y.; Matsumoto, K. *Nano Lett.* **2009,** *9,* 3318–3322.
252. Sofue, Y.; Ohno, Y.; Maehashi, K.; Inoue, K.; Matsumoto, K. *Jpn. J. Appl. Phys.* **2011,** *50,* 1.
253. Sardesai, N. P.; Barron, J. C.; Rusling, J. F. *Anal. Chem.* **2011,** *83,* 6698–6703.
254. Malhotra, R.; Patel, V.; Vaqué, J. P.; Gutkind, J. S.; Rusling, J. F. *Anal. Chem.* **2010,** *82,* 3118–3123.
255. Chikkaveeraiah, B. V.; Bhirde, A.; Malhotra, R.; Patel, V.; Gutkind, J. S.; Rusling, J. F. *Anal. Chem.* **2009,** *81,* 9129–9134.
256. Laird, E. D.; Wang, W.; Cheng, S.; Li, B.; Presser, V.; Dyatkin, B.; Gogotsi, Y.; Li, C. Y. *ACS Nano* **2012,** *6,* 1204–1213.
257. Zeng, G.; Xing, Y.; Gao, J.; Wang, Z.; Zhang, X. *Langmuir* **2010,** *26,* 15022–15026.
258. Zhao, J.; Chen, G.; Zhu, L.; Li, G. *Electrochem. Commun.* **2011,** *13,* 31–33.
259. Liu, P.; Zhang, X.; Feng, L.; Xiong, H.; Wang, S. *Am. J. Biomed. Sci.* **2011,** *3,* 69.
260. Yue, R.; Lu, Q.; Zhou, Y. *Biosens. Bioelectron.* **2011,** *26,* 4436–4441.
261. Rius-Ruiz, F. X.; Crespo, G. A.; Bejarano-Nosas, D.; Blondeau, P.; Riu, J.; Rius, F. X. *Anal. Chem.* **2011,** *83,* 5783–5788.
262. Zhao, X.; Kong, R.; Zhang, X.; Meng, H.; Liu, W.; Tan, W.; Shen, G.; Yu, R. *Anal. Chem.* **2011,** *83,* 5062.
263. Liu, M.; Zhao, H.; Chen, S.; Yu, H.; Zhang, Y.; Quan, X. *Chem. Commun.* **2011,** *47,* 7749.
264. Bucio, E.; Melendez-Ortiz, H. I.; Isoshima, T.; Macossay, J. Synthesis of Novel Stimuli Responsive Nanocomposite for Biomedical Applications. In *Recent Developments in Bio-nanocomposites for Biomedical Applications;* Tiwari, A., Ed.; Nova Science Pub Incorporated: Hauppauge, NY, 2010; pp 207–231.
265. Campuzano, S.; Wang, J. *Electroanalysis* **2011,** *23,* 1289–1300.

266. Wang, Y. T.; Yu, L.; Wang, J.; Lou, L.; Du, W. J.; Zhu, Z. Q.; Peng, H.; Zhu, J. Z. *J. Electroanal. Chem.* **2011,** *661,* 8–12.
267. Gao, R.; Zheng, J.; Zheng, X. *Microchim. Acta* **2011,** *174,* 273–280.
268. Mattinen, U.; Rabiej, S.; Lewenstam, A.; Bobacka, J. *Electrochim. Acta* **2011,** *56,* 10683–10687.
269. Bühlmann, P.; Chen, L. D. Ion-selective Electrodes with Ionophore-doped Sensing Membranes. In *Supramolecular Chemistry;* John Wiley & Sons, Ltd: Chichester, UK, 2012.
270. Li, J.; Yu, J.; Zhao, F.; Zeng, B. *Anal. Chim. Acta* **2007,** *587,* 33–40.
271. Male, K. B.; Hrapovic, S.; Luong, J. H. T. *Analyst* **2007,** *132,* 1254–1261.
272. Song, M.-J.; Kim, J.-H.; Lee, S.-K.; Lim, D.-S.; Hwang, S. W.; Whang, D. *Electroanalysis* **2011,** *23,* 2408–2414.
273. Wu, W.; Mitra, N.; Yan, E. C. Y.; Zhou, S. *ACS Nano* **2010,** *4,* 4831–4839.
274. Serafín, V.; Agüí, L.; Yáñez-Sedeño, P.; Pingarrón, J. M. *J. Electroanal. Chem.* **2011,** *656,* 152–158.
275. Liu, X. Y.; Zeng, X. D.; Mai, N. N.; Liu, Y.; Kong, B.; Li, Y. H.; Wei, W. Z.; Luo, S. L. *Biosens. Bioelectron.* **2010,** *25,* 2675–2679.
276. Kachoosangi, R. T.; Musameh, M. M.; Abu-Yousef, I.; Yousef, J. M.; Kanan, S. M.; Xiao, L.; Davies, S. G.; Russell, A.; Compton, R. G. *Anal. Chem.* **2009,** *81,* 435–442.
277. Xi, F.; Liu, L.; Wu, Q.; Lin, X. *Biosens. Bioelectron.* **2008,** *24,* 29–34.
278. Gopalan, A. I.; Lee, K.-P.; Ragupathy, D. *Biosens. Bioelectron.* **2009,** *24,* 2211–2217.
279. Xiao, F.; Zhao, F.; Zhang, Y.; Guo, G.; Zeng, B. *J. Phys. Chem. C* **2008,** *113,* 849–855.
280. Safavi, A.; Farjami, F. *Biosens. Bioelectron.* **2011,** *26,* 2547–2552.
281. Santhosh, P.; Manesh, K. M.; Uthayakumar, S.; Komathi, S.; Gopalan, A. I.; Lee, K. P. *Bioelectrochemistry* **2009,** *75,* 61–66.
282. Huang, H.-Y.; Chen, P.-Y. *Talanta* **2010,** *83,* 379–385.
283. Yang, M. H.; Choi, B. G.; Park, H.; Park, T. J.; Hong, W. H.; Lee, S. Y. *Electroanalysis* **2011,** *23,* 850–857.
284. Wu, H.-X.; Cao, W.-M.; Li, Y.; Liu, G.; Wen, Y.; Yang, H.-F.; Yang, S.-P. *Electrochim. Acta* **2010,** *55,* 3734–3740.
285. Ping, J.; Ru, S.; Fan, K.; Wu, J.; Ying, Y. *Microchim. Acta* **2010,** *171,* 117–123.
286. Bo, X.; Bai, J.; Yang, L.; Guo, L. *Sens. Actuators, B* **2011,** *157,* 662–668.
287. Fang, Y.; Guo, S.; Zhu, C.; Zhai, Y.; Wang, E. *Langmuir* **2010,** *26,* 11277–11282.
288. Zhu, H.; Liang, X.; Chen, J.; Li, M.; Zhu, Z. *Talanta* **2011,** *85,* 1592–1597.
289. Yang, J.; Zhang, W.-D.; Gunasekaran, S. *Biosens. Bioelectron.* **2010,** *26,* 279–284.
290. Liu, X.; Zhu, H.; Yang, X. *Talanta* **2011,** *87,* 243–248.
291. Lizeng, G.; Jie, Z.; Leng, N.; Jinbin, Z.; Yu, Z.; Ning, G.; Taihong, W.; Jing, F.; Dongling, Y.; Perrett, S.; Xiyun, Y. *Nat. Nanotechnol.* **2007,** *2,* 577–583.
292. Gao, L.; Zhuang, J.; Nie, L.; Zhang, J.; Zhang, Y.; Gu, N.; Wang, T.; Feng, J.; Yang, D.; Perrett, S.; Yan, X. *Nat. Nano* **2007,** *2,* 577–583.
293. Tang, J.; Tang, D.; Niessner, R.; Chen, G.; Knopp, D. *Anal. Chem.* **2011,** *83,* 5407–5414.
294. Zhang, L.; Yi, M. *Bioprocess Biosyst. Eng.* **2009,** *32,* 485.
295. Eguílaz, M.; Agüí, L.; Yáñez-Sedeño, P.; Pingarrón, J. M. *J. Electroanal. Chem.* **2010,** *644,* 30–35.
296. Liu, S.; Tian, J.; Wang, L.; Luo, Y.; Sun, X. *Analyst* **2011,** *136,* 4898.
297. Han, D.; Han, T.; Shan, C.; Ivaska, A.; Niu, L. *Electroanalysis* **2010,** *22,* 2001–2008.
298. Xue, Y.; Zhao, H.; Wu, Z.; Li, X.; He, Y.; Yuan, Z. *Biosens. Bioelectron.* **2011,** *29,* 102–108.
299. Zhang, Y.; Yuan, R.; Chai, Y.; Li, W.; Zhong, X.; Zhong, H. *Biosens. Bioelectron.* **2011,** *26,* 3977–3980.
300. Bao, Y.; Song, J.; Mao, Y.; Han, D.; Yang, F.; Niu, L.; Ivaska, A. *Electroanalysis* **2011,** *23,* 878–884.
301. Jia, D.; Ren, Q.; Sheng, L.; Li, F.; Xie, G.; Miao, Y. *Sens. Actuators, B* **2011,** *160,* 168–173.
302. Kavanagh, A.; Byrne, R.; Diamond, D.; Fraser, K. J. *Membranes* **2012,** *2,* 16–39.
303. Le Bideau, J.; Viau, L.; Vioux, A. *Chem. Soc. Rev.* **2011,** *40,* 907–925.
304. He, Y.; Lodge, T. P. *Chem. Commun.* **2007,** 2372–2734.
305. Ueki, T.; Watanabe, M. *Macromolecules* **2008,** *41,* 3739–3749.
306. Zhang, Y.; Zheng, J. *Electrochem. Commun.* **2008,** *10,* 1400–1403.
307. Zhang, J.; Lei, J.; Liu, Y.; Zhao, J.; Ju, H. *Biosens. Bioelectron.* **2009,** *24,* 1858–1863.
308. Usakli, A. B. *Comput. Intell. Neurosci.* **2010,** *2010.*
309. Marcilla, R.; Sanchez-Paniagua, M.; Lopez-Ruiz, B.; Lopez-Cabarcos, E.; Ochoteco, E.; Grande, H.; Mecerreyes, D. *J. Polym. Sci. Part A: Polym. Chem.* **2006,** *44,* 3958–3965.
310. Lopez, M. S.-P.; Mecerreyes, D.; Lopez-Cabarcos, E.; Lopez-Ruiz, B. *Biosens. Bioelectron.* **2006,** *21,* 2320–2328.
311. Jia, F.; Shan, C.; Li, F.; Niu, L. *Biosens. Bioelectron.* **2008,** *24,* 945–950.
312. Shan, C.; Yang, H.; Song, J.; Han, D.; Ivaska, A.; Niu, L. *Anal. Chem.* **2009,** *81,* 2378–2382.
313. Xiang, L.; Zhang, Z.; Yu, P.; Zhang, J.; Su, L.; Ohsaka, T.; Mao, L. *Anal. Chem.* **2008,** *80,* 6587–6593.
314. Lourenco, N. M. T.; Osterreicher, J.; Vidinha, P.; Barreiros, S.; Afonso, C. A. M.; Cabral, J. M. S.; Fonseca, L. P. *React. Funct. Polym.* **2011,** *71,* 489–495.
315. Nilsson, D.; Kugler, T.; Svensson, P.-O.; Berggren, M. *Sens. Actuators, B* **2002,** *86,* 193–197.
316. Khodagholy, D.; Curto, V. F.; Fraser, K. J.; Gurfinkel, M.; Byrne, R.; Diamond, D.; Malliaras, G. G.; Benito-Lopez, F.; Owens, R. M. *J. Mater. Chem.* **2012,** *22,* 4440–4443.
317. Curto, V. F.; Fay, C.; Coyle, S.; Byrne, R.; O'Toole, C.; Barry, C.; Hughes, S.; Moyna, N.; Diamond, D.; Benito-Lopez, F. *Sens. Actuators, B* **2012,** *171–172,* 1327–1334.
318. Curto, V. F.; Fay, C.; Coyle, S.; Byrne, R.; Diamond, D.; Benito-Lopez, F. Wearable Microfluidic PH Sweat Sensing Device Based on Colorimetric Imaging Techniques. In *The 15th International Conference on Miniaturized Systems for Chemistry and Life Sciences, μTAS 2011 (MicroTAS) Conference, Seattle, USA;* 2011.
319. Wan, Q.; Yu, F.; Zhu, L.; Wang, X.; Yang, N. *Talanta* **2010,** *82,* 1820–1825.
320. Xiao, F.; Zhao, F.; Zeng, J.; Zeng, B. *Electrochem. Commun.* **2009,** *11,* 1550–1553.
321. Ng, S. R.; Guo, C. X.; Li, C. M. *Electroanalysis* **2011,** *23,* 442–448.
322. Ohtani, T.; Nishi, N.; Kakiuchi, T. *J. Electroanal. Chem.* **2011,** *656,* 102–105.
323. Jia, J.; Cao, L.; Wang, Z.; Wang, T. *Electroanalysis* **2008,** *20,* 542–549.
324. Michalska, A. *Electroanalysis* **2012,** *24,* 1253–1265.
325. Ash, P. A.; Vincent, K. A. *ChemInform* **2012,** *43.*
326. Alva, S. *J. Diabetes Sci. Technol.* **2008,** *2,* 546–551.
327. Vallée-Bélisle, A.; Plaxco, K. W. *Curr. Opin. Struct. Biol.* **2010,** *20,* 518–526.
328. Justino, C. I. L.; Rocha-Santos, T. A.; Duarte, A. C. *TrAC Trends Anal. Chem.* **2010,** *29,* 1172–1183.
329. Mishra, A. K.; Mishra, S. B.; Tiwari, A.; Rai, R. S. Fabrication of Bionanocomposites from Natural Biopolymer Matrices and Inorganic Nanofillers. In *Recent Developments in Bio-nanocomposites for Biomedical Applications;* Tiwari, A., Ed.; Nova Science Pub Incorporated: Hauppauge, NY, 2010; pp 173–190.
330. Kadokawa, J.-i.; Murakami, M.-a.; Kaneko, Y. *Carbohydr. Res.* **2008,** *343,* 769–772.
331. Kopecek, J. *J. Polym. Sci. Part A: Polym. Chem.* **2009,** *47,* 5929–5946.
332. Lodge, T. P. *Science* **2008,** *321,* 50–51.
333. Seiffert, S.; Sprakel, J. *Chem. Soc. Rev.* **2012,** *41,* 909–930.
334. Pasparakis, G.; Vamvakaki, M. *Polym. Chem.* **2011,** *2,* 1234–1248.
335. Kuksenok, O.; Yashin, V. V.; Balazs, A. C. *Soft Matter* **2009,** *5,* 1835–1839.

336. Magin, C. M.; Cooper, S. P.; Brennan, A. B. *Mater. Today* **2010,** *13,* 36–44.
337. Scardino, A. J.; de Nys, R. *Biofouling* **2010,** *27,* 73–86.
338. Bhandari, P.; Narahari, T.; Dendukuri, D. *Lab Chip* **2011,** *11,* 2493–2499.
339. Hu, L.; Pasta, M.; Mantia, F. L.; Cui, L.; Jeong, S.; Deshazer, H. D.; Choi, J. W.; Han, S. M.; Cui, Y. *Nano Lett.* **2010,** *10,* 708–714.
340. Dhende, V. P.; Samanta, S.; Jones, D. M.; Hardin, I. R.; Locklin, J. *ACS Appl. Mater. Interfaces* **2011,** *3,* 2830–2837.
341. Lee, S.-K.; Kim, B. J.; Jang, H.; Yoon, S. C.; Lee, C.; Hong, B. H.; Rogers, J. A.; Cho, J. H.; Ahn, J.-H. *Nano Lett.* **2011,** *11,* 4642–4646.
342. Kim, D. H.; Lu, N. S.; Ma, R.; Kim, Y. S.; Kim, R. H.; Wang, S. D.; Wu, J.; Won, S. M.; Tao, H.; Islam, A.; Yu, K. J.; Kim, T. I.; Chowdhury, R.; Ying, M.; Xu, L. Z.; Li, M.; Chung, H. J.; Keum, H.; McCormick, M.; Liu, P.; Zhang, Y. W.; Omenetto, F. G.; Huang, Y. G.; Coleman, T.; Rogers, J. A. *Science* **2011,** *333,* 838–843.
343. Carta, R.; Jourand, P.; Hermans, B.; Thoné, J.; Brosteaux, D.; Vervust, T.; Bossuyt, F.; Axisa, F.; Vanfleteren, J.; Puers, R. *Sens. Actuators, A* **2009,** *156,* 79–87.
344. Windmiller, J. R.; Bandodkar, A. J.; Valdes-Ramirez, G.; Parkhomovsky, S.; Martinez, A. G.; Wang, J. *Chem. Commun.* **2012,** *48,* 6794–6796.
345. Bandodkar, A. J.; Hung, V. W. S.; Jia, W.; Valdes-Ramirez, G.; Windmiller, J. R.; Martinez, A. G.; Ramirez, J.; Chan, G.; Kerman, K.; Wang, J. *Analyst* **2013,** *138,* 123–128.